AIMS Mathematics

http://www.aimspress.com/journal/Math

AIMS Mathematics, 8(2): 4487–4523.
DOI:10.3934/math.2023223
Received: 09 September 2022
Revised: 11 November 2022
Accepted: 17 November 2022
Published: 05 December 2022

Research article

Modeling variants of the COVID-19 virus in Hawai‘i and the responses to forecasting

Richard Carney[1], **Monique Chyba**[1,*], **Victoria Y. Fan**[2], **Prateek Kunwar**[1], **Thomas Lee**[2,3,], **Ionica Macadangdang**[1] **and Yuriy Mileyko**[1]

[1] Department of Mathematics, University of Hawai‘i at Mānoa, 2565 McCarthy Mall Honolulu, Hawai‘i 96822

[2] Thompson School of Social Work & Public Health, University of Hawai‘i at Mānoa, Honolulu, HI 96822, USA

[3] Hawaii Data Collaborative, Honolulu, HI 96813, USA

* **Correspondence:** Email: chyba@hawaii.edu; Tel: +1-201-616-0621; Fax: +1-808-956-9139.

Abstract: In this paper we introduce a model for the spread of COVID-19 which takes into account competing SARS-CoV-2 mutations as well as the possibility of reinfection due to fading of vaccine protection. Our primary focus is to describe the impact of the B.1.617.2 (Delta) and B.1.1.529 (Omicron) variants on the state of Hawai‘i and to illustrate how the model performed during the pandemic, both in terms of accuracy, and as a resource for the government and media. Studying the effect of the pandemic on the Hawaiian archipelago is of notable interest because, as an isolated environment, its unique geography affords partially controlled travel to and from the state. We highlight the modeling efforts of the Hawai‘i Pandemic Applied Modeling Work Group (HiPAM) which used the model presented here, and we detail the model fitting and forecasting for the periods from July 2021 to October 2021 (Delta surge) and from November 2021 to April 2022 (Omicron surge). Our results illustrate that the model was both accurate when the forecasts were built on assumptions that held true, and was inaccurate when the public response to the forecasts was to enforce safety measures that invalidated the assumptions in the model.

Keywords: COVID-19; epidemiological compartmental model; multi-variants; vaccines; reinfection; state of Hawai‘i
Mathematics Subject Classification: 39Axx, 92D25, 92D30, 93-10

1. Introduction

A primary focus of our paper is to present a more complete compartmental model for the spread of the coronavirus disease 2019 (COVID-19). There is a plethora of writings regarding mathematical modeling applied to the current pandemic. A reader interested in a comprehensive review may consult [3], which is a book dedicated to investigating mathematical techniques for the modeling and simulation of the Covid-19 viral pandemic, and references therein. Our model incorporates competing variants of the virus along with fading of vaccine protection, and a possibility of reinfection when an infected individual becomes susceptible again. Indeed, as viruses continue to circulate, they adapt to their changing environment through mutations. The latter occur when a virus replicates itself, since errors can be made during the RNA or DNA replication process. Beneficial (to the virus) mutations persist and accumulate, eventually resulting in a copy which can be sufficiently distinct from the original virus so as to exhibit different characteristics [13]. If this occurs, the copy is considered a variant strain of the original virus. Such changes in the viral genome may prolong their survival in hosts through increased transmissibility or improved immune system evasion, for instance. A virus variant exhibiting these traits along with a decreased effectiveness of prevention or treatment response, increased virulence, or detrimental changes in COVID-19 epidemiology at a global health scale, is what the World Health Organization (WHO) defines as a COVID-19 Variant of Concern (VOC). As of January 2022, WHO identified five VOCs: Alpha, Beta, Gamma, Delta and Omicron. In this paper we focus on the impact of the latter two variants on the state of Hawai‘i. Pharmaceutical measures such as vaccinations can drastically impact the evolution of a pandemic, which was indeed the case for COVID-19. However, it has been confirmed that individuals might become reinfected after their immunity from a prior infection starts waning [37]. Therefore, a comprehensive and accurate model needs to account for all of these specific features, i.e. COVID-19 models had to evolve alongside with the pandemic. For the past two years, the model described below has been used to fit data for the state of Hawai‘i, provide forecasts, and serve as a resource to the state in its fight against the severe acute respiratory syndrome coronavirus 2 (SARS-CoV-2). Indeed, mathematical models have been central to the public and policy debate throughout the COVID-19 pandemic [2]. Modeling provides an important tool to characterize, for instance, the impact of the pandemic on the healthcare system or school safety. More generally, it helps to explore various intervention strategies and assess their efficacy. See [36] for a case study on the Republic of Mauritius, another Island nation, and [39] on an extended SEIR model to incorporate the effect of testing, tracing and isolation.

Figure 1 shows major milestones for the evolution of the global pandemic over the first two years, with explicit appearances of the Delta and Omicron variants, and the beginning of implementation of vaccines. A Hawai‘i specific timeline can be found in Figure 5 in Section 3.

In response to the emergency of the pandemic, the Hawai‘i Pandemic Applied Modeling Work Group (HiPAM) was created at the University of Hawai‘i. The group was composed of health care workers, epidemiologists, data scientists, and many others working together with the goal of helping the state of Hawai‘i. This was done by providing mathematical and data driven tools that could inform decision-making and state planning. Modeling and forecasting have been a core part of HiPAM's mission, and it relied heavily on the model which is essentially the one presented here. HiPAM has been committed to frequently updating model designs and specifications and the resulting forecasts in order to adapt and account for the many unique qualities of Hawai‘i among the 50 States. In particular,

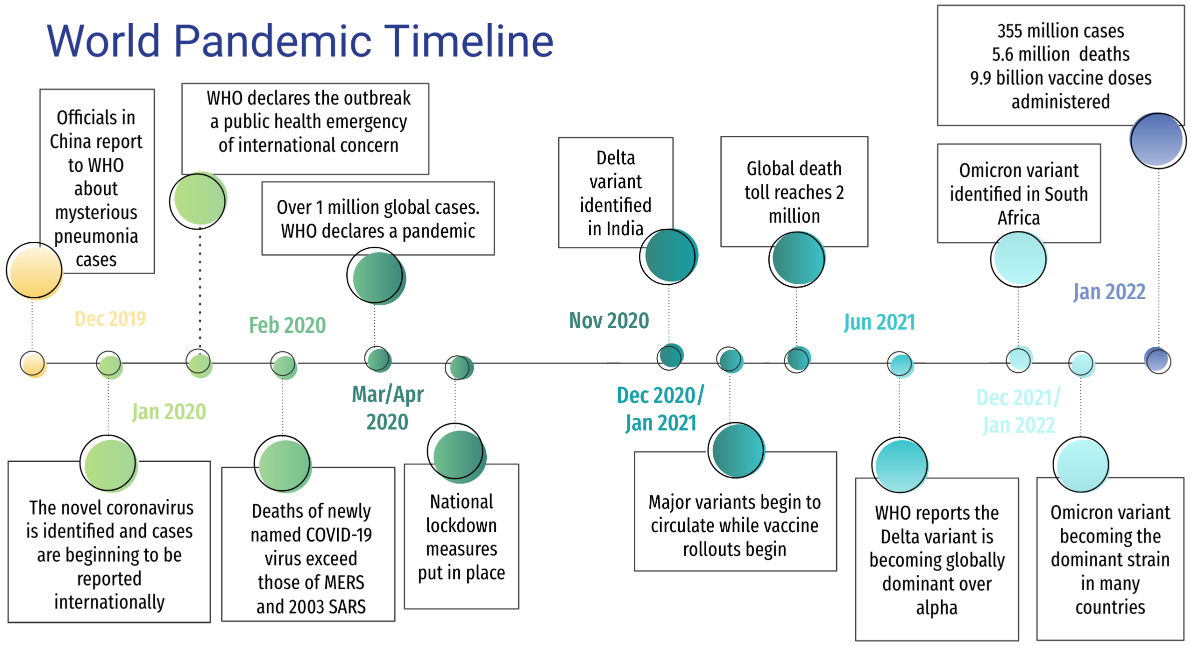

Figure 1. World's Timeline of the COVID-19 pandemic from end of 2019 to early 2022.

the HiPAM website [18] was updated at least once a week for a significant portion of the pandemic up until the summer of 2022. The updates displayed the latest available data for COVID-19 daily new cases, active hospitalizations and ICU beds, total deaths, and active cases. In addition, the model described in this paper (albeit a simplified version) was used to provide three two week forecasts for each set of data: a best-case, worst-case, and estimated prediction for how the numbers could change in time. The website is also a repository for the frequent HiPAM reports that incorporated the more sophisticated modeling approach we describe in this paper, and provided the interested parties along with the general public with the latest forecasting efforts and the most up to date analysis of where Hawai'i stood in the progress of the pandemic.

The outline of the paper is as follows. Section 2 provides a detailed description of our discrete compartmental model. Section 3 introduces Hawai'i specific features that need to be taken into account by the model. In Section 4, the focus is shifted to the model performance after vaccinations became available and new variants of concern started to emerge, including several HiPAM reports that were produced using the model. Section 5 offers a discussion regarding our modeling efforts and concludes the paper.

2. Compartmental model including travelers, vaccine and reinfection

Compartmental models, sometimes called equation based models (EBMs) have been widely used in epidemiological modeling for over a century, starting with the work of Ross (1916) [35], Ross and Hudson (1917) [34], Kermack and McKendrick (1927) [26] and Kendall (1956) [25], all in the effort to study infectious diseases. In [28] the authors compare compartmental modeling with another common approach, agent based modeling (ABMs), listing pros and cons of each approach. For this paper we focus solely on a compartmental model tailored to the Hawaiian Islands in particular. For a standard SEIR approach, the population is partitioned into four compartments based on the status therein of individuals' relationship to the disease: susceptible, exposed, infected, or removed. Each compartment relates to the others via differential equations, or as here, difference equations which have been discretized by each day. A common assumption that is typically made, as it is here, is that the total population size (sum over all compartments) is fixed and the populous within each compartment is homogeneous relative to infection and spread of the disease, as seen in [5, 10–12, 19, 27, 44].

Because of the simplicity of a four compartment model, we can make precise statements about what are the possible results, but on the other hand, we fail to capture all the different factors that are at play in reality. The possible outcomes of a virus spreading within a population are inherently dependent on the choices and actions of the people, and so a four compartment partition is too coarse and needs refining in order to capture more nuanced possibilities. Hence, we push the setup further, and include new modifications, e.g. sub-compartments to represent individuals with distinct characteristics like travelers visiting the islands, or health care workers who are more likely to be exposed, but also may behave more cautiously in social situations. Additionally, we include the most common mitigation and preventative measures i.e. protection from wearing masks as well as a fifth compartment corresponding to the individuals who have received a dosage of a vaccine. In particular, our SEIR model setup for COVID-19 may differ from a classical model in that the exposed category, corresponding to infected individuals without symptoms, does not lead exclusively into the infected category of symptomatic individuals. Rather, we allow infected yet asymptomatic individuals to bypass the I category via an outgoing arrow directly from E to R. This is an important distinction since this is not always assumed, but we know for COVID-19 that an infected individual will not always show symptoms and therefore will potentially spread the virus in a way that differs from an individual who is aware they are sick. The reader may refer to the work in [8] for more details.

Our earliest modeling efforts were originally inspired by [29], which subsequently led to [7], published at the beginning stages of the pandemic and developed prior to the vaccinations or the threat of more variants. When more unique circumstances to Hawaiʻi became relevant, the model was expanded as seen in [9]. This paper focuses on three further developments to the model, each meant to capture an important factor of the pandemic which plays a significant part in the reality of the disease spread. First, we generalize the approach for incorporating any number, K, of variant strains as they appear in the population, since important parameter values may differ between them. This allows us to account for differences in rate of infection, hospitalization rate, etc. Second and third are the import realities of vaccine fading and the possibility of re-infection. While it is true that contracting the virus and then recovering will likely boost one's natural immunity, it is also true that infection can happen again after a relatively short period of time. Therefore, an individual making it through the model into the recovered compartment should not indefinitely prevent them from rejoining the susceptible compartment. Similarly, the efficacy of the vaccines will wane over time, which is why booster shots have been such an important part of Hawaiʻi State's vaccination efforts. Including vaccine fading is important if one wishes to gain insight into the potential effect of future vaccination efforts.

2.1. *Discrete generalized SEIR model*

Our model is an extension of the model presented in [9], which is a discrete compartmental model with time steps of one day. Here we assume that the population is exposed to some number $K \geq 1$ of different variants. When referring to an arbitrary one of these variants, we use a subscript or superscript k. The compartments S, V, E, I and R represent susceptible, vaccinated susceptible, asymptomatic, symptomatic, and recovered populations, respectively. We neglect birth and death rates since they are marginal in comparison to the total population which we therefore assume constant. For our simulations, death can be calculated by taking a percentage of hospitalized individuals (which can be variant dependent). It is important to note that in our model, the diagram and equations below actually exist for 3 different sub-groups: $c, h,$ and v representing the general community, healthcare workers, and visitors, respectively. If we refer to travelers, we are thinking of both tourists and returning residents. The returning residents are added to the c subgroup (community) because they are expected to behave the same as the larger community, whereas the tourists are treated as having a different behaviour. Hence, in what follows, by v we denote the travelers who are classified as tourists.

The compartments $\bar{E}$ and $\bar{I}$ represent the asymptomatic and symptomatic populations who are vaccinated. That is, a compartment marked with a bar contains individuals who have the full protection from vaccination. We assume that the latter occurs after completing vaccination regardless of, for example, booster shot status or the brand of the vaccine. Also, individuals are assumed to have completed vaccination if they received at least two doses of the vaccine, except for the Johnson and Johnson vaccine for which a single shot is sufficient. Vaccine fading is introduced in the model through a pathway from V to S, which we assume happens uniformly for all individuals after θ days, assuming they never became sick. The possibility of re-infection is implemented in the model via pathways from each R^k, the recovered compartment for the k-th variant, into the S and V compartments, depending on the individuals' vaccination status. In other words, we ensure that when a recovered individual once again becomes susceptible, their vaccination status is retained. While the susceptible and vaccinated susceptible pool is shared between all the variants, each variant has a distinct E^k, I^k, and R^k (and the applicable bar) compartment. This means that each individual can only be asymptomatic or symptomatic with one variant at a time and that an individual who recovers from a variant will eventually become susceptible again and possibly re-infected with either the same variant or another one. In Figure 2 we provide a high level structure of a multi-variant SEIR model.

Equation (2.1) represents the dynamics of the susceptible compartment. NV here stands for "newly vaccinated" and is a list of real data values collected from the department of Health, with individual entries $NV(t)$ corresponding to the number of newly vaccinated individuals on day t. The values of $NV(t)$ may vary as t changes, or it may stay constant for some time, as the data required may not be readily available, in which case $NV(t)$ may be set to a constant that approximates the average rate of vaccination.

$$S(t+1) = S(t) - \left(\sum_{k=1}^{K} (1 - e^{-\lambda_k(t)}) S(t) \right) - NV(t) + \zeta(t,\theta) NV(t-\theta) + \sum_{k=1}^{K} \psi_k(t) R^k(t) \tag{2.1}$$

Then similarly we have vaccinated individuals:

$$V(t+1) = V(t) - \left(\sum_{k=1}^{K} (1 - e^{-\lambda_k(t)}) \mu_k V(t) \right) + NV(t) - \zeta(t,\theta) NV(t-\theta) + \sum_{k=1}^{K} \Psi_k(t) R^k(t) \tag{2.2}$$

To determine the number of susceptible individuals on day $t+1$ we start with those who were susceptible on day t. Next we subtract from this $\sum_{k=1}^{K} (1 - e^{-\lambda_k(t)}) S(t)$, which is the number of individuals

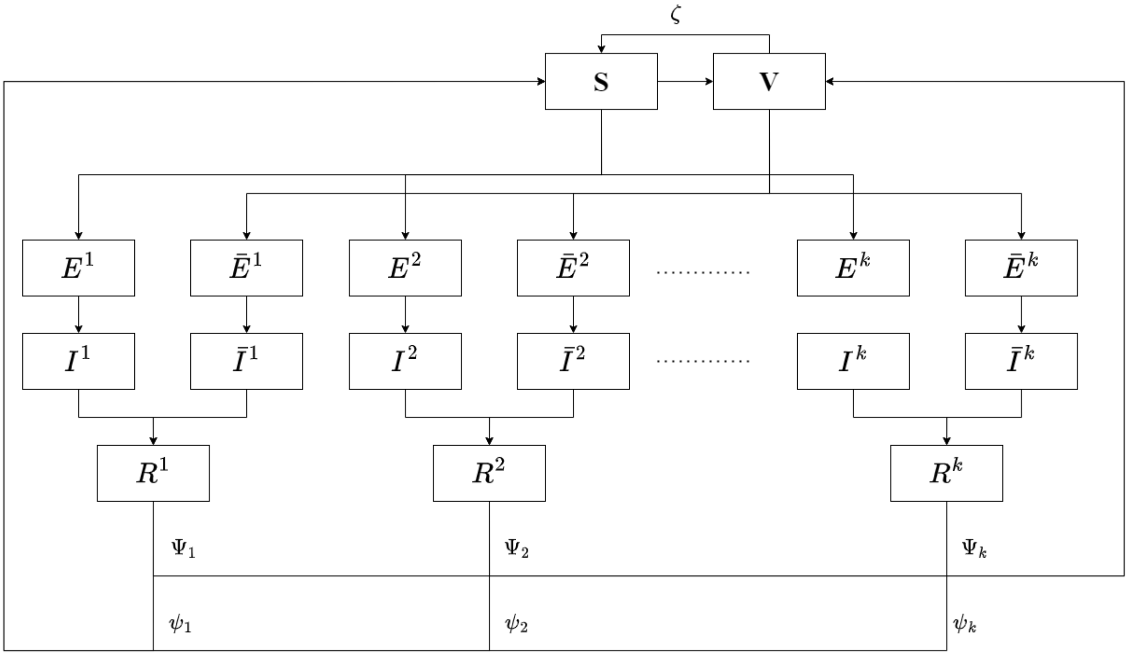

Figure 2. High Level Structure of Multi Variant SEIR model with vaccine fading and re-infection. Subscript k is used to distinguish variants, ζ represents vaccine fading, ψ_k and Ψ_k are the proportion of recovered individuals (unvaccinated and vaccinated respectively) who become susceptible again. The compartments E^k and I^k are further subdivided into 14 and 5 sub-compartments respectively. The E_k compartment is partitioned into fourteen sub-compartments to account for the possibility of individuals remaining asymptomatic for some period of time or never develop symptoms (14 represents a two weeks length of asymptomatic illness before recovering). I_k is sub-divided into 5 sub-compartments to account different level of symptoms severity. More details can be found in Figure 2 of [28].

who were infected by any one of the K variants on day t. Then we subtract the newly vaccinated individuals $NV(t)$, but also we add back $\zeta(t,\theta)NV(t-\theta)$, representing the effect of vaccine fading, where $\zeta(t,\theta) = \prod_{i=1}^{\theta}\prod_{k=1}^{K}(1-\mu_k(1-e^{-\lambda_k(t-\theta+i)}))$. In other words, we put back the individuals who were subtracted from S as newly vaccinated θ days ago, where θ days is the time it takes a vaccinated person to become more or less fully susceptible again according to best current evidence, assuming that they were never infected with any of the K variants. For simplicity in our simulations we take $\zeta = 0.6$, as the formula becomes unwieldy when the number of variants increases, and furthermore it is unknown whether vaccine fading should be dependent on the brand of vaccine, for example, or if it should truly apply to all individuals equally and in the same amount of time. The equation to determine the number of vaccinated susceptible on day $t+1$ is structurally the same as that for susceptible, except that the newly vaccinated individuals are added and the individuals losing their vaccine protection are subtracted. In addition, we use μ_k to denote the reduced susceptibility in vaccinated individuals for the kth variant. Since vaccinations provide protection in two different ways - reducing transmissibility and susceptibility, the latter of which is difficult to estimate, we use $\mu_k = 1$ for most of the simulations and the effect of vaccination is achieved via reduced transmissibility. However, we have the flexibility to adjust this value. The time dependent parameters $\psi_k(t)$ and $\Psi_k(t)$ in (2.1) and (2.2) represents the proportion of non-vaccinated and vaccinated individuals, respectively, who recovered from variant k become susceptible to re-infection again. These proportions are calculated as $\psi_k(t) = \frac{E_0^k(t-\theta_k)}{R^k(t)}$ and $\Psi_k(t) = \frac{\bar{E}_0^k(t-\bar{\theta}_k)}{R^k(t)}$ where we take θ_k and $\bar{\theta}_k$ days according to best current evidence.

Following equations (2.1) and (2.2), we begin to describe the equations for an arbitrary variant k from the set of all K variants. Importantly, the structure of the equations remains the same for all the variants, with the only difference being potentially the parameter values. Therefore, the dependence on k is suppressed below, but every parameter value may potentially depend on k. In [9, 28] one can find detailed diagrams of the earlier versions of the model. The parameters are explained in Table 1 and parameter values used for our simulations are also provided in that same table. As before, we still have three groups per equation that are not explicitly shown for brevity: $c-$community, $h-$healthcare, and $v-$visitors. Equations (2.3) and (2.4) describe the dynamics for the compartment E_0 (resp. $\bar{E}_0$ for vaccinated) representing individuals that just got infected. They are assumed to be asymptomatic on the first day of infection.

$$E_0(t+1) = (1 - e^{-\lambda(t)})S(t) \tag{2.3}$$

$$\bar{E}_0(t+1) = (1 - e^{-\lambda(t)})\mu V(t) \tag{2.4}$$

The rest of the dynamics for asymptomatic and symptomatic individuals is linear and we use matrix notation to describe it. Let $Q(t) = (E_1, \cdots, E_{13}, I_0, \cdots, I_4)^T$, with $Q_q(t)$, $\bar{Q}(t)$, $\bar{Q}_q(t)$ the corresponding vectors for quarantined/isolated and vaccinated populations. We have

$$Q(t+1) = \begin{pmatrix} 1-p_0 \\ 0 \\ \vdots \\ p_0 \\ 0 \\ \vdots \\ 0 \end{pmatrix} (1 - q_{a,0})E_0(t) + MQ(t) \tag{2.5}$$

where

$M = A \bigoplus B$, $A = \begin{pmatrix} 0_{1\times 12} & 0 \\ D & 0_{12\times 1} \\ \mathbf{s} & s_{13} \end{pmatrix}$, $\bigoplus$ being the matrix direct sum, with $D = \mathrm{Diag}[(1-p_i)(1-q_{a,i})]_{i=1,12}$, $\mathbf{s} = (s_i)^T_{i=1,12}$, $s_i = p_i(1 - q_{a,i})$, for $i = 1, \ldots, 13$, and

$$B = \begin{pmatrix} 1-q_{s,0} & 0 & 0 & 0 & 0 \\ 0 & 1-q_{s,1} & (1-r_2)(1-q_{s,2}) & 0 & 0 \\ 0 & 0 & r_2(1-q_{s,2}) & (1-r_1)(1-q_{s,3}) & 0 \\ 0 & 0 & 0 & r_2(1-q_{s,3}) & (1-r_1)(1-q_{s,4}) \end{pmatrix} \tag{2.6}$$

For the isolated symptomatic and quarantined asymptomatic, we have

$$Q_q(t+1) = \begin{pmatrix} 1-p_0 \\ 0 \\ \vdots \\ p_0 \\ 0 \\ \vdots \\ 0 \end{pmatrix} (q_{a,0}E_0(t) + E_{q,0}(t)) + M_{q1}Q(t) + M_{q2}Q_q(t) \tag{2.7}$$

$M_{q1} = A_q \bigoplus B_q$, $A_q = \begin{pmatrix} 0_{1\times 12} & 0 \\ D_q & 0_{12\times 1} \\ \mathbf{s}_q & s_{q,13} \end{pmatrix}$ with $D_q = \mathrm{Diag}[(1-p_i)q_{a,i}]_{i=1,12}$, $\mathbf{s}_q = (s_{q,i})^T_{i=1,12}$, $s_{q,i} = p_i q_{a,i}$ and

$$B_q = \begin{pmatrix} q_{s,0} & 0 & 0 & 0 & 0 \\ 0 & q_{s,1} & (1-r_2)q_{s,2} & 0 & 0 \\ 0 & 0 & r_2 q_{s,2} & (1-r_1)q_{s,3} & 0 \\ 0 & 0 & 0 & r_2 q_{s,3} & (1-r_1)q_{s,4} \end{pmatrix} \tag{2.8}$$

and finally by construction we also have $M_{q2} = (A + A_q) \bigoplus (B + B_q)$. For the vaccinated populations, the dynamics are identical except for possible adjustment to the parameters p_i and r_i that will be written $\bar{p}_i$ and $\bar{r}_i$ in the sequel. Note that asymptomatic individuals move daily through 14 days of illness unless they develop symptoms or quarantine themselves. On the other hand, symptomatic individuals can stay in some of the stages of the illness progressing for several days (the rate of progression is denoted by r_2). As mentioned earlier, the dynamics for the vaccinated populations are similar with the exception of the parameter values representing the rates for asymptomatic individuals to become symptomatic, i.e. p_i coefficients depend on the vaccination status and are therefore represented by $\bar{p}_i$. In our model the rate of isolation is assumed to be the same for both non-vaccinated and vaccinated populations, but it could be generalized to account for a possibly different behavior. In Figure 3 we display a schematic for the interaction between isolated and non-isolated symptomatic individuals.

Finally, Equation (2.9) expresses the dynamics of the recovered compartment:

$$\begin{aligned} R(t+1) = {} & (1-\psi(t))R(t) + r_1(I_4(t) + I_{q,4}(t)) + \bar{r}_1(\bar{I}_4(t) + \bar{I}_{q,4}(t)) + (r_1 - r_2)(I_3(t) + I_{q,3}(t)) \\ & + (\bar{r}_1 - \bar{r}_2)(\bar{I}_3(t) + \bar{I}_{q,3}(t)) + (1-p_{13})(E_{13}(t) + E_{q,13}(t)) + (1-\bar{p}_{13})(\bar{E}_{13}(t) + \bar{E}_{q,13}(t)), \end{aligned} \tag{2.9}$$

where we assume that an individual can recover by staying asymptomatic for 14 days, or from stages 3 and 4 of the illness when having symptoms.

Next, we provide the expressions for the hazard rate, λ. Note that this rate is variant as well as group dependent. First, we calculate the total population for our three groups, which are community, health care workers and visitors, denoting these quantities by N_c, N_h, and N_v, respectively:

$$N_v(t) = S_v(t) + V_v(t) + \sum_{k=1}^{K} (E_v(t) + I_v(t) + R_v(t)) \tag{2.10}$$

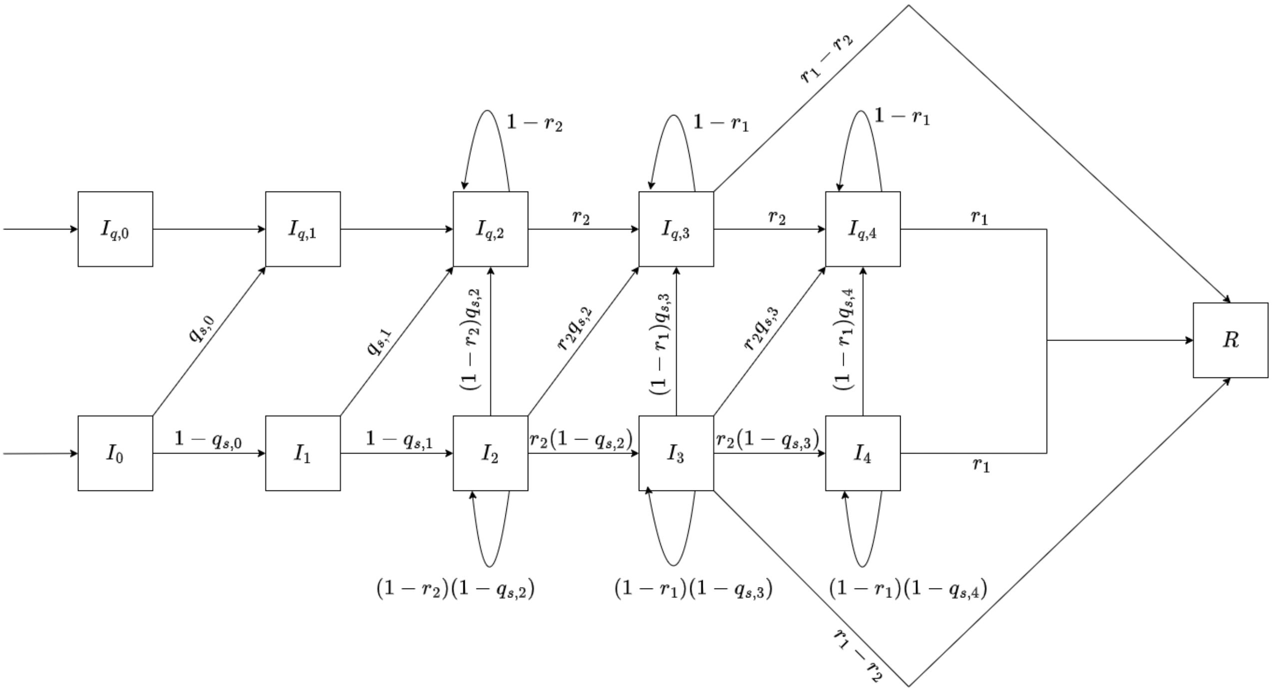

Figure 3. In the above diagram shows the flow in the I,I_q sub compartments. The flow between sub-compartments for vaccinated population is the same with each sub-compartment being replaced by it's bar version, the rate from $\bar{I}_{q,3}$ to $\bar{I}_{q,4}$ being r_3 instead of r_2 and the rate from $\bar{I}_{q,3}$ to Recovered compartment being $r_1 - r_3$ instead of $r_1 - r_2$.

$$N_h(t) = S_h(t) + V_h(t) + \sum_{k=1}^{K} (E_h(t) + I_h(t) + R_h(t)) \tag{2.11}$$

$$N_c(t) = S_c(t) + V_c(t) + \sum_{k=1}^{K} (E_c(t) + I_c(t) + R_c(t)) + \rho_h N_h(t) + \rho_v N_v(t) \tag{2.12}$$

where ρ_h, ρ_v represent the mixing ratios between the different groups.

Now we use the above quantities to normalize the hazard rates. We note again that there are three hazard rates for each value of k, and the dependence on k is suppressed for convenience:

$$\lambda_c(t) = \tilde{\beta}\Big[Z_c(t) + \omega\bar{Z}_c(t) + \sum_{\alpha\in\{h,v\}} \rho_\alpha(Z_\alpha(t) + \omega\bar{Z}_\alpha(t))\Big]/N_c \tag{2.13}$$

where $\tilde{\beta} = \beta(1 - p_{mp}(1 - p_{me}))\Omega_{\text{vaccpass}}\mho_{\text{factor}}$, $Z_\alpha = I_\alpha(t) + \varepsilon E_\alpha(t) + \gamma((1-\nu)I_{\alpha,q} + \varepsilon E_{\alpha,q})$, and the coefficients are described in Table 1 and Table 2.

Similarly we have the hazard rates for the healthcare workers and the visitors:

$$\lambda_h(t) = \rho_h\lambda_c + \tilde{\beta}\Big[Z_h(t) + \omega\bar{Z}_h(t)]\Big]/N_h \tag{2.14}$$

$$\lambda_v(t) = \rho_v\lambda_c + \tilde{\beta}\Big[Z_v(t) + \omega\bar{Z}_v(t)]\Big]/N_v \tag{2.15}$$

Certain quantities used in our simulations are not governed by separate dynamics. Rather, they are computed as closed form expressions involving other quantities. In particular, two important estimates obtained from the model are the number of active hospitalizations and the number of new daily infections. The former is calculated by summing up specific fractions of the sizes of compartments $I_3, I_4, I_{q,3}$, and $I_{q,4}$, essentially regarding the corresponding sub-populations as individuals who have progressed to severe stages of the disease. These fractions, often referred to as hospitalization rates, vary throughout the course of the pandemic and across the counties. The values used in the model are given in Tables 5 and 9, where the rate of hospitalization for the population in stage four is twice the rate of hospitalization for the population in stage three. The daily number for active hospitalizations is computed as:

$$Hosp(t) = \sum_{k=1}^{K} (\sigma_1 H_3 + \sigma_2 H_4) \tag{2.16}$$

where $H_i = \sum_{\alpha\in\{c,h,v\}} \left(I_{\alpha,i} + \bar{I}_{\alpha,i} + I_{\alpha,q,i} + \bar{I}_{\alpha,q,i}\right)$, and σ_1, σ_2 are the hospitalization rates.

The number of daily new infections is calculated using the following formula:

$$Ni(t) = \sum_{k=1}^{K} \left(Ni_I + Ni_E + (1-r)q_{s,13}I_{13} + (1-r)q_{s,13}\bar{I}_{13}\right) \tag{2.17}$$

where $Ni_I = \sum_{\alpha\in\{c,h,v\}} \left(\sum_{i=0}^{i=12} \left(q_{s,i}(I_i + \bar{I}_i)\right)\right)$ and $Ni_E = \sum_{\alpha\in\{c,h,v\}} \left(\sum_{i=0}^{i=12} \left(q_{a,i}(E_i + \bar{E}_i)\right)\right)$.

2.2. *Parameters and assumptions*

In Tables 1 and 2 we provide explanation for the values for the parameters used in the model and the values we used for the simulations.

3. Controlled geographic location - Hawaiian archipelago

In this paper we focus on the islands in the Hawaiian archipelago. It consists of eight islands, of which seven are inhabited. The state of Hawai‘i is divided into five counties: Honolulu, Hawai‘i, Maui, Kaua‘i and Kalawao, of which the last has an extremely small population. Therefore, we model the first four counties with assumed populations shown in Table 3 that account for over ninety-nine percent of the state's population. The geographically closed borders and uniform mitigation measures make the Hawaiian islands a controlled environment, interesting for study. To read more about the unique history of disease in the state of Hawai‘i, see [24].

When studying an island chain like Hawai‘i, an important factor to consider, which is not applicable to the other 49 States, stems from the state's ability to partially control individuals' movements in and out of the islands. Relatively quickly after the first confirmed case, the state perceived an urgent need to adopt and implement effective mitigation strategies in order to control the spread of the disease and eventually to bring it to a halt. First, in order to stop the influx of new SARS-CoV-2 infections into the state by travelers, a 14 day quarantine for all travelers was put in place on March 26, 2020, and was extended to inter-island travel on April 1, 2020. A former daily average of 30,000 tourist arrivals was reduced to only about one hundred. The traveling restrictions were relaxed on October

Table 1. Parameters intrinsic to COVID-19 [6, 7, 23, 30, 31]**: This is due to the fact that by December 2020 all healthcare workers were vaccinated and we assume they behave like community members then. Note that some parameters depend on geographic location, demographics and other variables. They can therefore not all be found in the literature and some were estimated specifically for Hawai‘i using our model fit.

Parameter, meaning	**Value**
β, basal transmission rates	optimized to fit data
Factors modifying transmission rate	
ε, asymptomatic transmission (25% reduction in transmission)	0.75 (could be variant dependent)
ρ_h, reduced healthcare worker interactions	0.8, until December 2020 and then 1.0**
ρ_v, reduced visitor interactions	0.5
γ, quarantine and isolation (80% reduction in transmission)	0.2
κ, hospital precautions	0.5
η, healthcare worker precautions	0.2375
Population fractions (assumed constant but could potentially be variant dependant)	
p_i, i =0,...,13, rate of onset of symptoms after day i	0.000792, 0.00198, 0.1056, 0.198, 0.2376, 0.0858, 0.0528, 0.0462, 0.0396, 0.0264, 0.0198, 0.0198, 0.0198, 0
$q_{s,i}$, i =0,...,4, rate of symptomatic isolation after day/stage i	C: 0.1, 0.4, 0.8, 0.9, 0.99; H: 0.2, 0.5, 0.9, 0.98, 0.99
$q_{a,i}$, i =0,...,13, rate of asymptomatic quarantine after day/stage i	0.0, 0.0, 0.0, 0.0, 0.0, 0.05, 0.05 0.05, 0.0, 0.0, 0.0,0.0, 0.0, 0.0
$r_1, \bar{r}_1$, rate of recovery for unvaccinated and vaccinated population	0.2
$r_2, \bar{r}_2$, rate of transition to severe stage of infection for unvaccinated and vaccinated	0.085
θ_k, delay for possibility of re-infection for k^{th} variant	210 days
ν, reduced transmission of symptomatic hospitalized individuals	0.11

15, 2020 with the introduction of the safe travel program, which allowed individuals with a negative test from an approved partner taken within 72 hours of arrival to skip the 14 day quarantine. The role of travelers is critical in the modeling, as they are the only means of new viral spread within the closed populations. Furthermore, the ratio of travelers to residing residents varies greatly between the islands, potentially leading to significant differences in the outcomes, a fact which needs to be

Table 2. Parameters intrinsic to vaccination used in our simulations [32, 33, 41]. Note that some parameters depend on geographic location, demographics and other variables. They can therefore not all be found in the literature and some were estimated specifically for Hawai'i using our model fit.
*: This simplification was made because the reduction in susceptibility is difficult to estimate and the protection provided by vaccine is achieved through other parameters.
**: The choice of the value 0.6 for the parameter ζ is based on the estimate that, at the time of introduction of vaccine fading in the model, about 40% of individuals in Hawai'i who were fully vaccinated had also received the (first) booster dose. This leaves 60% of the vaccinated individuals vulnerable to losing their immunity due to vaccine fading effects. In addition, we assume the same distribution for booster dose as we had observed for vaccination.

Parameter, meaning	Value
Factors modifying transmission rate	
ω, reduced transmissibility due to vaccination	0.20 before Omicron and 0.24 afterwards
μ_k, reduced susceptibility for k^{th} variant	1 *
$\bar{p}_i$, $i = 0, 1, ...13$, probability of onset of symptoms after day i (after vaccination)	0.000492, 0.001080, 0.002056, 0.0415, 0.002376, 0.000858, 0.000528, 0.000302, 0.00019, 0.00019, 0.00019, 0.00019, 0.00019, 0
$\Omega_{vaccpass}$, reduced susceptibility due to Vaccine Passport	0.6 for duration of safe access Oahu on Honolulu county only
$\mho_{factor}$, increased transmissibility for variants	Varies by variant
ζ, vaccine fading factor	0.6**
θ, vaccine fading delay	180 days
NV, vaccinations received per day	Varies by geographic location and time, as shown in Figure 6

taken into account. As mentioned previously, we make a distinction between the returning residents, who mix with the community as they enter the state, and tourists, who we refer to as visitors. We refer the reader to [28] for a more precise schematic of how the incoming travelers are incorporated, and to [9] for the data used to design the model. Finally, the Hawai'i safe travel program was ended on March 25, 2022 for all counties. After this date, travel restrictions are removed from the model and travelers are divided between vaccinated and unvaccinated compartments according to the U.S. average. International travelers do still require vaccination to enter the U.S. but they form a relatively small percentage of incoming travelers. Figure 4 displays the travelers input used for our model, it is based on data from [40] and approximated by a piecewise constant function over two weeks intervals. It can be observed that Maui County has the largest ratio of travelers versus residents while Honolulu County has the smallest. The county of Kaua'i had extremely low detected cases of infections until

May 2020 and the model could not be applied before that date, that is why travelers are shown only for May 2020 and beyond. It can be observed that in Spring 2022 the number of travelers for the County of Kauaʻi significantly increased, which is mostly due to a return of tourists similar to pre-pandemic levels.

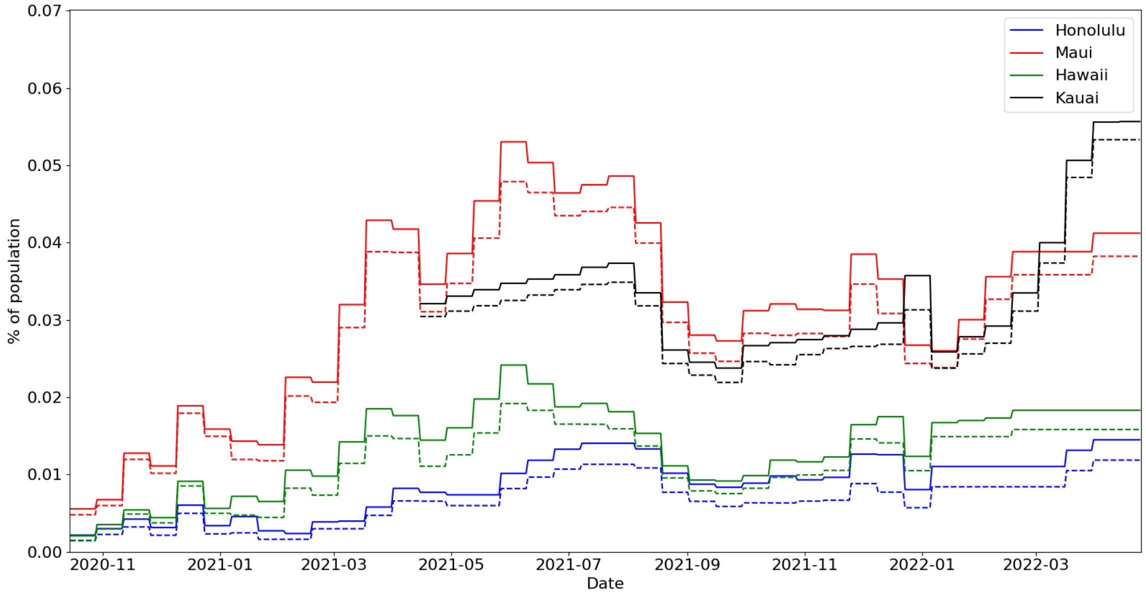

Figure 4. Evolution of traveler arrival in the state of Hawaiʻi as percentage of total population per day over time for each county. The solid line represents a total travelers per day and the dotted line represents the total visitors per day. The difference between the two are returning residents.

In Figure 5 we show a timeline of the pandemic in Hawaiʻi up until January 2022, displaying the main milestones and mitigation measures taken. It can be observed that during the first year of the pandemic many public policies put in place underwent significant changes, making it somewhat difficult for the state to properly implement such policies, and quite challenging for the population to adequately abide by them. For the time period we focus on in this paper, there were some key changes in mitigation strategies, but comparatively less than in the early stages of the pandemic. For example, the indoor mask mandate ended on March 25, 2022 coinciding with the end of the safe travel program, with Hawaiʻi being the last of the 50 States to lift the restrictions. However, it is clear that a non-trivial amount of masking remains, for instance, when riding public transit, or at UH Manoa, where teachers are still required to wear masks while lecturing (at the time of writing this paper, masks mandates have since been dropped).

The contained environment offered by the Islands of Hawaiʻi is ideal for us to study the differences in the impact of variants. More details can be found in [9]. Delta and Omicron mutations have especially dominated in the state of Hawaiʻi. The Delta variant B.1.617.2 was first identified in India in December of 2020, but as of June 21, 2021 there were just 13 known cases in the state of Hawaiʻi. The Omicron variant B.1.1.529 was first identified nearly a year later in Botswana in November of 2021, and in Hawaiʻi only about a month later. Notably the Omicron strain was more infectious but

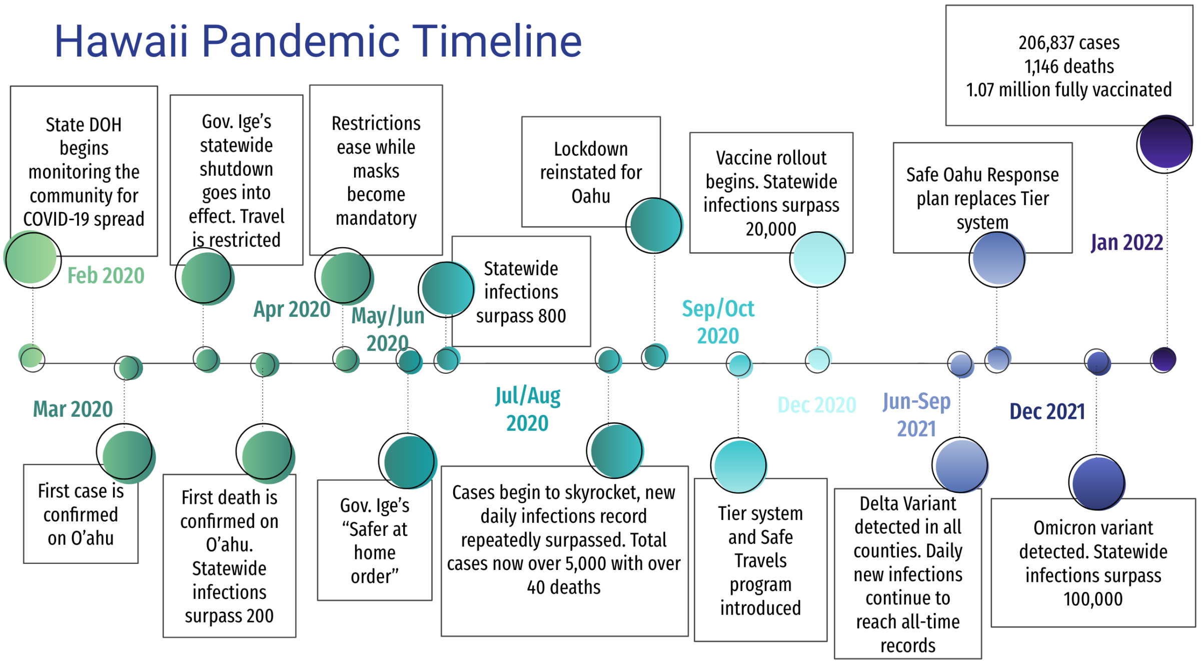

State DOH begins monitoring the community for COVID-19 spread

First case is confirmed on O'ahu

Gov. Ige's statewide shutdown goes into effect. Travel is restricted

First death is confirmed on O'ahu. Statewide infections surpass 200

Restrictions ease while masks become mandatory

Gov. Ige's "Safer at home order"

Statewide infections surpass 800

Cases begin to skyrocket, new daily infections record repeatedly surpassed. Total cases now over 5,000 with over 40 deaths

Lockdown reinstated for Oahu

Tier system and Safe Travels program introduced

Vaccine rollout begins. Statewide infections surpass 20,000

Delta Variant detected in all counties. Daily new infections continue to reach all-time records

Safe Oahu Response plan replaces Tier system

Omicron variant detected. Statewide infections surpass 100,000

206,837 cases
1,146 deaths
1.07 million fully vaccinated

Figure 5. Hawai'i's Timeline of the COVID-19 pandemic for years 2020 and 2021.

with milder symptoms as compared to Delta.

For our simulations, parameter values are estimated from known data shown in Tables 1, 2 and 3, with the exception of the basal transmission rate, β, which is chosen numerically to minimize the error between the model's output and some true data values. In the earliest stages of the pandemic, the data used for model fitting were the numbers for new daily cases (see [9] for the data used). Later on, however, data availability and accuracy came under question due to at-home tests becoming readily available as well as the slow down in data reporting, as the data that were previously reported each day were now reported weekly. After this, the number of active hospitalizations was taken as a more useful gauge of the model's accuracy.

Table 3. Susceptible population for each county and first detected case [14,42,43]. Note that we restricted Honolulu County to O'ahu Island only.

Region	$S_c(0)$	$S_h(0)$	Date for $I_{c,0}(0) = 1$
Honolulu	937,711	15000	March 6, 2020
Hawai'i	201,513	1500	March 16, 2020
Maui	167,417	1500	March 15, 2020
Kaua'i	72,143	150	April 15, 2021

4. Simulations for the counties of the state of Hawai'i

In this paper we focus on the second phase of the pandemic, when vaccination was implemented and we started seeing new variants spreading around the world. Simulations, results and discussions for the Hawaiian Islands during the first phase of the pandemic, which we refer to as the period prior to vaccination, can be found in [7, 9, 28]. The model fit with respect to real data is discussed in those papers as well. We focus here on the period from December 2020, when vaccines became available, to April 2022. During this time period our model was used as a reference and resource by the Governor Office, the Healthcare Association of Hawai‘i, and the hospitals. HiPAM had a heavy presence in news media to communicate with the public the role of the model and simulations. Forecast reports were generated to inform leaders involved in decision making, and educational videos were produced for the public. All of the resources were distributed by HiPAM and are accessible on its website [18]. In the next few sections we describe the results of the model fit and forecasts as they occurred during the progression of the pandemic. To better highlight the effect of the vaccination on the spread of the virus several initial figures show the pre-vaccination numbers along with the ones during the vaccination period.

4.1. Vaccination implementation starting in December 2020

The Hawai‘i Department of Health (DOH) started COVID-19 vaccinations on December 15, 2020. A state vaccination distribution plan was drafted and can be found on the website [16]. One year later, by December 15, 2021, 2, 439, 075 COVID-19 vaccine doses had been administered in Hawai‘i. DOH estimated then that 73.2% of the state's population had received either two doses of the Pfizer or Moderna vaccine or one shot of the Johnson & Johnson vaccine. Figure 6 shows the input function $NV(t)$ used for our model. It is approximated based on real data and was adjusted every time a significant change in vaccination rates was detected. A higher rate of vaccination can be observed until about May 2021, i.e. for the first 5 months of the campaign, with all counties plateauing now. It is interesting to see that Kaua‘i county was initially the most aggressive in its vaccination program to then start plateauing earlier than the other counties, with a very small vaccination increase since August 2021. Our model fit for daily cases is represented in Figures 7, 8 and 9 for the counties of Honolulu, Hawai‘i and Maui. Cases were too small in the County of Kaua‘i and the model could not be run for that time period. The period is limited from March 6, 2020 (first case detected in Hawai‘i) to June 30, 2021 before the appearance of the new Delta variant. The red rectangles represent the

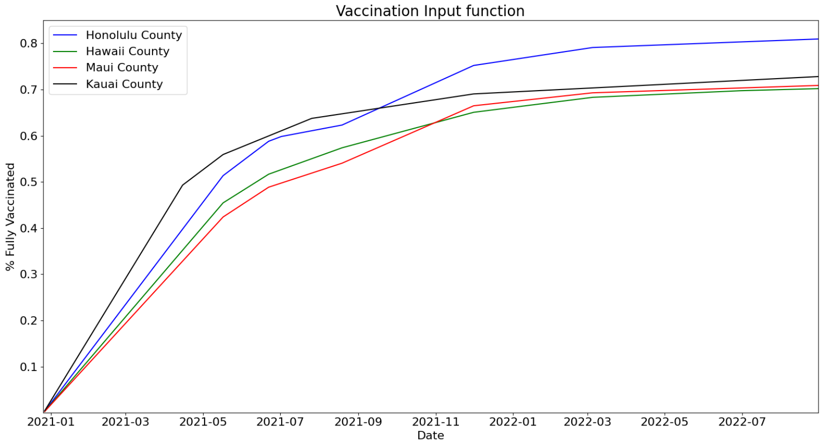

Figure 6. Vaccine Input function $NV(t)$ from December 27, 2020 to August 31. Vaccinations as of September 3, 2022 are Hawai‘i: 69%, Maui: 71%, Kaua‘i: 73% and Honolulu: 80%.

basal transmission rate β, the changes correspond to the actual non-pharmaceutical mitigation taken in the different counties such as lockdown, mask mandate, safe travel, etc. Other parameters are fixed and were not used to optimize the fit. No new variant with significant difference in transmission was introduced until the Alpha variant B.1.1.7. in April 2021, so we assume $\mho_{factor} = 1$ from March 6, 2020 to March 30, 2021 and $\mho_{factor} = 1.3$ from April 1, 2021 to account for the appearance of the Alpha variant B.1.1.7 in the Islands (we use 1.3 instead of 1.5 since infections were a combination of the original variant and the Alpha one). There is then a gradual change of $\mho_{factor}$ from May 15, 2021 to July 8, 2021 to account for the appearance of the Delta variant, see Section 4.2 for more details. We compute the discrete L_2 distance to measure the error of the model fit compared to the DOH reported data for the three counties, see Table 4. The real data and the model fit are both normalized using the maximal value of the detected daily cases (it can be found in the captions of Figures 7 to 9). As expected, the error is quite reduced when comparing to the 7-day average since compartmental models average the behavior of the population groups. It is not surprising to see that the best fit is for Honolulu county since it has the largest population and number of reported daily cases. Hawai‘i and Maui counties have larger errors, which is due to more drastic relative variation in reported daily cases than for the Honolulu County.

Table 4. L_2 distance to measure the error of the model fit with respect to real data.

County	L_2 distance between model fit and actual data	L_2 distance between model fit and 7 day average of actual data
Honolulu	0.284	0.191
Hawai‘i	0.319	0.223
Maui	0.334	0.230

It can be observed on Figure 7 that Honolulu had its largest surge and number of reported cases during August 2020, which prompted the State to reintroduce a lockdown (for all counties). The introduction of the safe travel program on October 15, 2020 generated a new surge that was flattened with the start of the vaccination program in the state in December 2020. Maui followed a different trajectory which can be attributed to a slower rate of vaccination and a larger increase in travelers when compared to the other counties, see Figures 6 and 4, respectively. The largest transmission rate occurred for all three counties during the initial surge in March, which was countered rapidly with a severe lockdown. In June 2021, the spread of the virus seemed to be under control in the state of Hawai‘i, which resulted in some relaxation of mitigation measures as the vaccines prevented the surge in infections. Unfortunately, the Delta variant B.1.617.2, which has disrupted this trend, was already detected, although in a small number of cases.

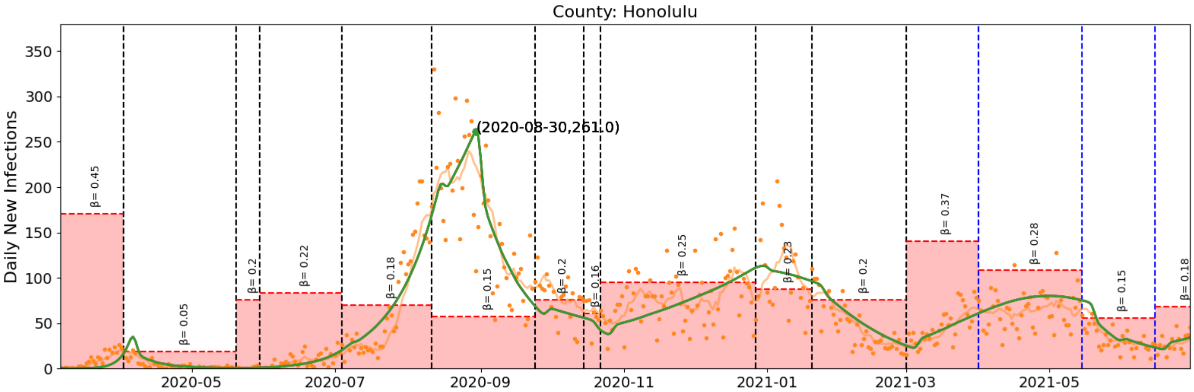

Figure 7. Honolulu County fit. The orange dots are the daily cases reported by the DOH, and the green line corresponds to the model fit with corresponding β's in red. The largest value for detected cases was 330 individuals on August 12, 2020. Black vertical lines correspond to adjustment of β (due to mitigation measures or change in people's behavior) and blue vertical lines correspond to changes in $\mho_{factor}$.

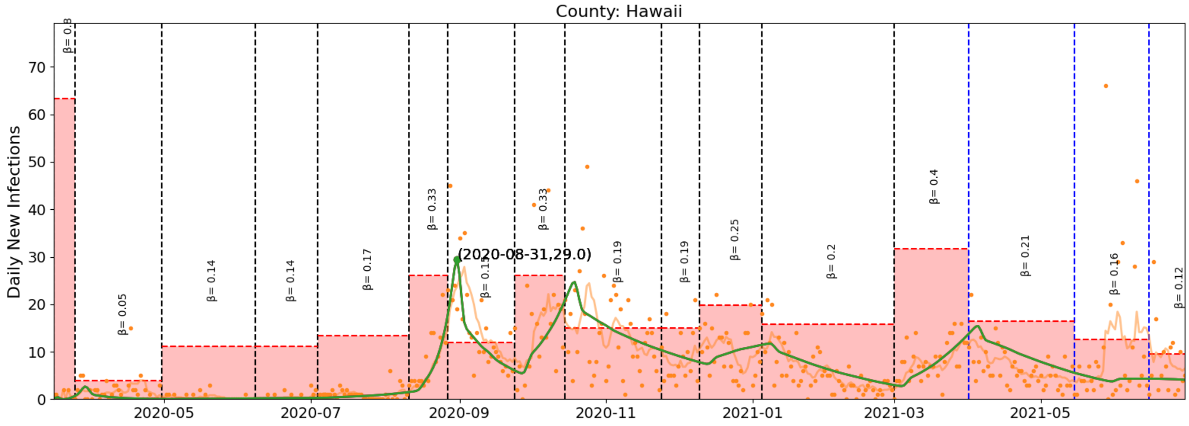

Figure 8. Hawai'i County fit. The orange dots are the daily cases reported by the DOH, and the green line corresponds to the model fit with corresponding β's in red.The largest value for detected cases was 66 individuals on May 28, 2021. Black vertical lines correspond to adjustment of β (due to mitigation measures or change in people's behavior) and blue vertical lines correspond to changes in $\mho_{factor}$.

4.2. *Delta variant B.1.617.2*

Mutations started to be a real cause for concern with the appearance of a new variant called Delta Variant B.1.617.2. Daily cases increased rapidly, doubling in the U.S. as of July 13, 2021 compared to June 23, 2021. The first available variant report by the DOH in the state of Hawai'i was on June 9, 2021, and they have been released about every 2 weeks since [15]. On June 19, 2021 the DOH reported that from a pool of specimens from positive samples analyzed by genomic sequencing 19% were the

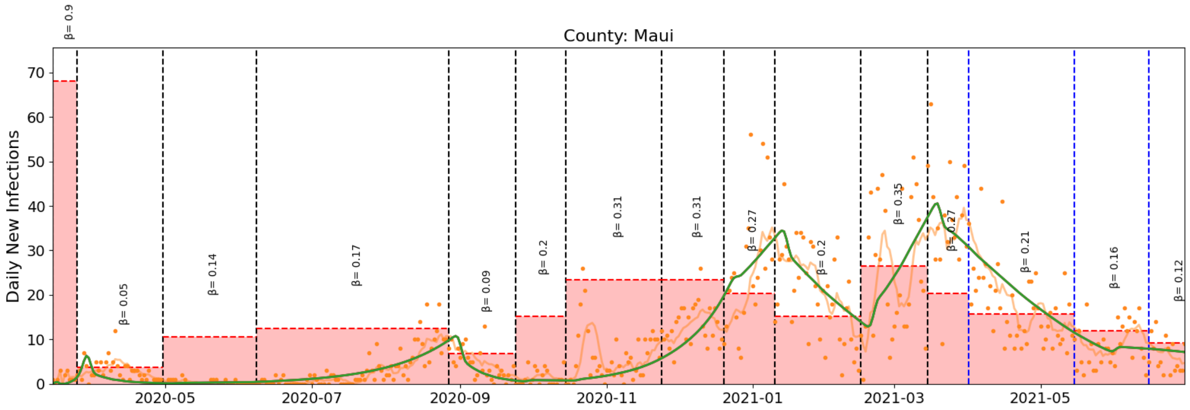

Figure 9. Maui County fit. The orange dots are the daily cases reported by the DOH, and the green line corresponds to the model fit with corresponding β's in red.The largest value for detected cases was 63 individuals on March 16, 2021.

Delta Variant B.1.617.2, with this number growing to 55% on July 3, 2021 and then to 74% on July 31, 2021. In Mid-July all variant cases were observed to have been declining over the prior three months, except for the Delta variant whose numbers were increasing. Delta was completely dominant in the state of Hawai‘i as of August 14, 2021. Bar graphs representing the changes in variant distribution among analyzed samples can be found in [15]. Since early summer of 2020 was the beginning of the largest surge in Honolulu County experienced between the beginning of the pandemic and June 2021, on July 29, 2021 our team produced a report comparing the new daily infections between the periods of June-July 2020 and June-July 2021, see Figure 10. It can be observed that cases were slightly above in 2021, but most importantly, the growth was much more pronounced in July, suggesting an alarming trend. Because in general the spread of a disease follows an exponential growth and decay, it might be very difficult to assess the beginning of a new surge and the gravity of it.

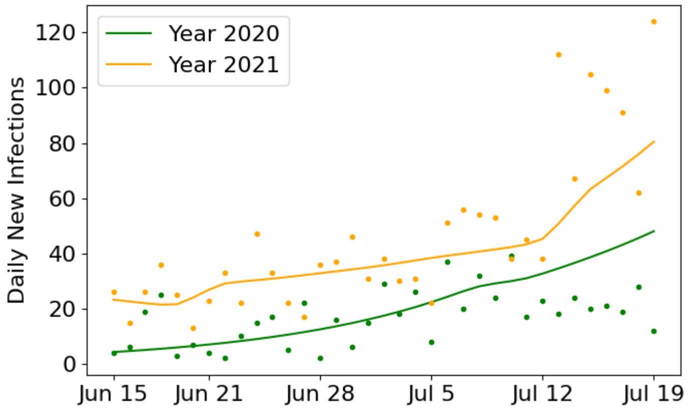

Figure 10. Daily New Cases in 2020 vs. 2021. The dot are the reported data by the DOH while the curves represent the model fit during the dates in year 2020 and year 2021.

Based on data from various sources, B.1.617.2 is estimated in our model to be about 50% more transmissible than the Alpha variant B.1.1.7. At the time of the appearance of Delta B.1.617.2 the model was not designed for competing variants, therefore another approach was taken to implement the transition from the original Alpha variant to the Delta mutation. We used the model described in Section 2 with a single variant, i.e. $K = 1$, but varying $\mho_{factor}$ over a seven weeks period from May 15,2021 to July 8, 2021 going up from 1.3 to 2.2 (about 1.5^2 more transmissible than the original variant). Delta became dominant rapidly, the ramping up of $\mho_{factor}$ accounts for the mixing of variants during a few week period.

The first simulations were designed to demonstrate the impact of vaccination on flattening the curve. It is illustrated in Figure 11 for Honolulu County and showed that to avoid an increase to more than 200 detected daily new cases, the percentage of the vaccinated population in the county would need to reach 80%. For each curve we assume that vaccination is stopped completely once the levels reach 65%, 70% and 80% respectively. Such simulations were used as educational messaging for the public to encourage vaccination. Important is also the observation that for about a month of the early stage of the surge the dynamics of the new daily cases is identical in all three scenarios, despite a very different outcome for a longer forecast. This could result in actions being taken too late. The black dots in Figure 11 represent the actual data collected afterwards. It can be seen that while at first they are above the forecast, they start trending down starting in early September. This was due to newly imposed mitigation measures rather than reaching the goal of 80% vaccination level, since the actual vaccination level was at around 65%. So, the blue curve in Figure 11 shows the projection for the daily cases without the new mitigation measures. It highlights the fact that flattening of the curve can occur through various actions.

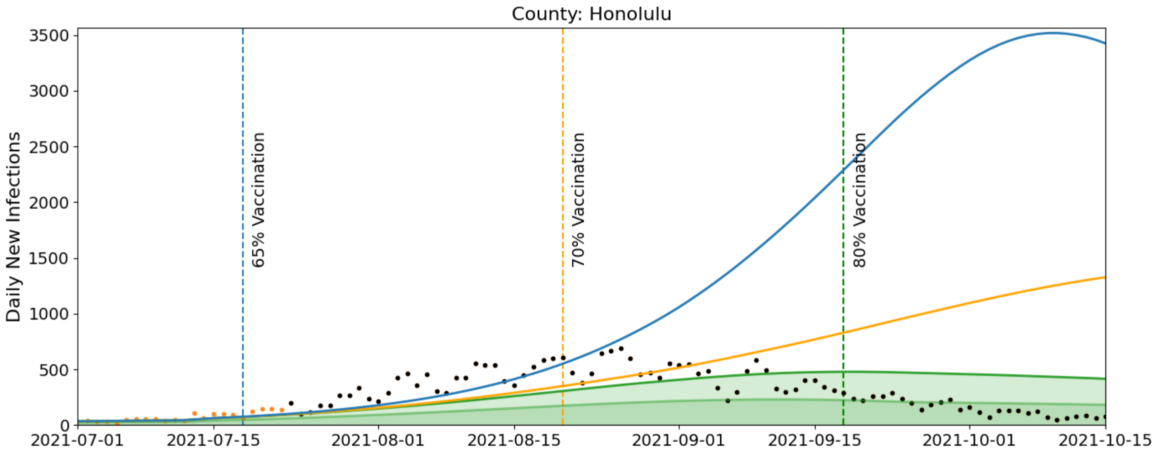

Figure 11. Scenarios for different vaccination level. The blue curve assumes 65% of the Honolulu county vaccinated on July 18, 2021, orange curve assumes reaching 70% on August 20, 2021 and the green one (scenario 3) reaching 80% on September 18, 2021. The light green shaded area corresponds to the fractions of detected daily cases predicted by the model in scenario 3 for vaccinated individuals while the dark shaded area is for unvaccinated. The orange dots represent the data that was available at the time of forecasting and the black dots are the actual data that became available since then.

On August 15, 2021 our team provided a forecast of new daily cases assuming that the percentage of the vaccinated population will stay constant after reaching the levels shown in the Figure 11 as 65%, 70% and 80%, and no new mitigation measures were to be implemented, see Figure 12. The forecast was 3,614 on September 25 for new daily cases and largely above the critical threshold of about 400 active hospitalizations for Honolulu County, after which the health system would get overwhelmed and would not function normally. The forecast was shared with the government and media outlets, and newspaper articles starting raising the alarm, see e.g. [20]. As a result, mitigation measures were promptly imposed. In particular, Honolulu County announced a four-week suspension of all large gatherings to begin August 25, 2021, restricting events to 25 people outdoors and 10 indoors. On September 13, this was followed by the safe access program, which required all employees, contractors, and volunteers of businesses, such as restaurants, bars, gyms, and movie theaters to show proof of full vaccination against COVID-19 or a negative COVID-19 test result each week, in order to operate. Fortunately, these measures proved effective in making the model prediction an over-estimate, as people's adjusted behaviors acted as feedback and cases started trending downward to eventually stabilize in October 2021.

The two week lag between active hospitalizations and new daily cases can be clearly observed from the figures. Hospitalization parameters used for this forecast is the first line of Table 5 for the entire duration, since the later adjustments were made after the fact. Despite successfully flattening the curve for new daily cases, hospitalization numbers were still alarmingly high and additional measures were necessary. For example, the state had to tap into its emergency ventilator stockpile [17], began canceling elective surgeries, and had to divert patients with emergency health needs to other hospitals [21, 22].

Figures 13 to 16 display the evolution of the spread of the virus during the Delta period, July 1, 2021 to October 15, 2021. In Table 5, the hospitalization parameters are provided. It can be seen that model hospitalization rates for symptomatic individuals in stages 3 and 4 of the disease, (σ_1, σ_2), decreased, mostly noticeably for Honolulu County, which is a consequence of the fact that Honolulu had a high number of cases and vaccinated individuals would stay asymptomatic or would have only very mild symptoms.

Table 5. Hospitalization rates(σ_1, σ_2) for four counties.

Dates (2021)	Honolulu(σ_1, σ_2)	Hawai'i(σ_1, σ_2)	Maui(σ_1, σ_2)	Kaua'i(σ_1, σ_2)
July 8-Aug 15	(9%,18%)	(4.5%,9%)	(4.5%,9%)	(4.5%,9%)
Aug 16-Sep 1	ramp down	(4.5%,9%)	ramp down	ramp down
Sep 2-Sep 15	(7%,14%)	(4.5%,9%)	ramp down	(2%,4%)
Sep 16-Oct 1	ramp down	(4.5%,9%)	(4%,8%)	(2%,4%)
Oct 2-Nov 1	(5%,10%)	(4.5%,9%)	(4%,8%)	(2%,4%)

As can be seen in Figure 13, Honolulu County had a surge that peaked around the end of August and was followed by a steady decline down to under 200 reported daily cases by mid-October. It can be observed that the fit for active hospitalizations was quite accurate. Since those data do not depend on testing there is less fluctuations for Honolulu county which has the largest numbers of all counties. The day with the largest number of active hospitalizations was in early September. The distances between the model fit and the reported data, both for new daily cases and active hospitalizations, as well as

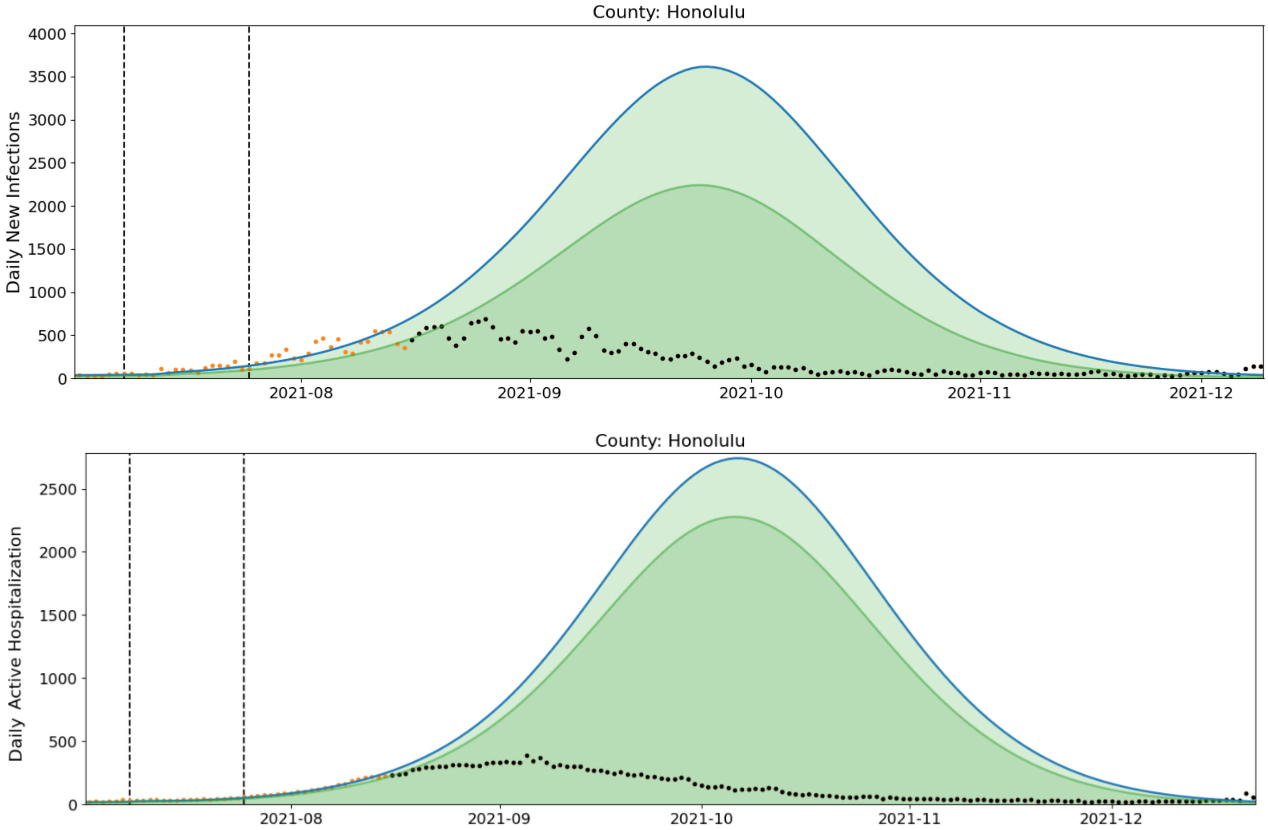

Figure 12. Top plot is projected daily cases if no mitigation measures were taken and bottom plot is corresponding projected active hospitalization. The light green shaded region represents the vaccinated population and the dark shaded represents the unvaccinated. The orange dots represent the actual cases as was available at the time of projection and the black dots represent the daily cases that were reported since then. Highest value for hospitalization is forecast to be 2743 on October 6 and for new infections is forecast to be 3614 on September 25.

between the model fit and the corresponding 7 day averages of the data, are shown in Table 6, where the data is normalized by the max values indicated in the caption of Figure 13 - Figure 16.

The spread of the disease for the same time period for the other counties can be seen in Figures 14, 15 and 16. All counties display the same trend as Honolulu County, a peak at the end of August followed by a decline until mid-October. The relative decrease in basal transmission β due to mitigation and adjustment of public behavior was 36% for Honolulu, 56% for Hawai‘i and 48%, 49% for Maui and Kaua‘i, respectively. It can be seen that the model fit for active hospitalization is not very good for Kaua‘i, the model providing values above the reported data by the DOH. This might come from the fact that Kaua‘i has a very limited health care capabilities (very few ventilators for instance) and individuals might be flown to other facilities in Honolulu.

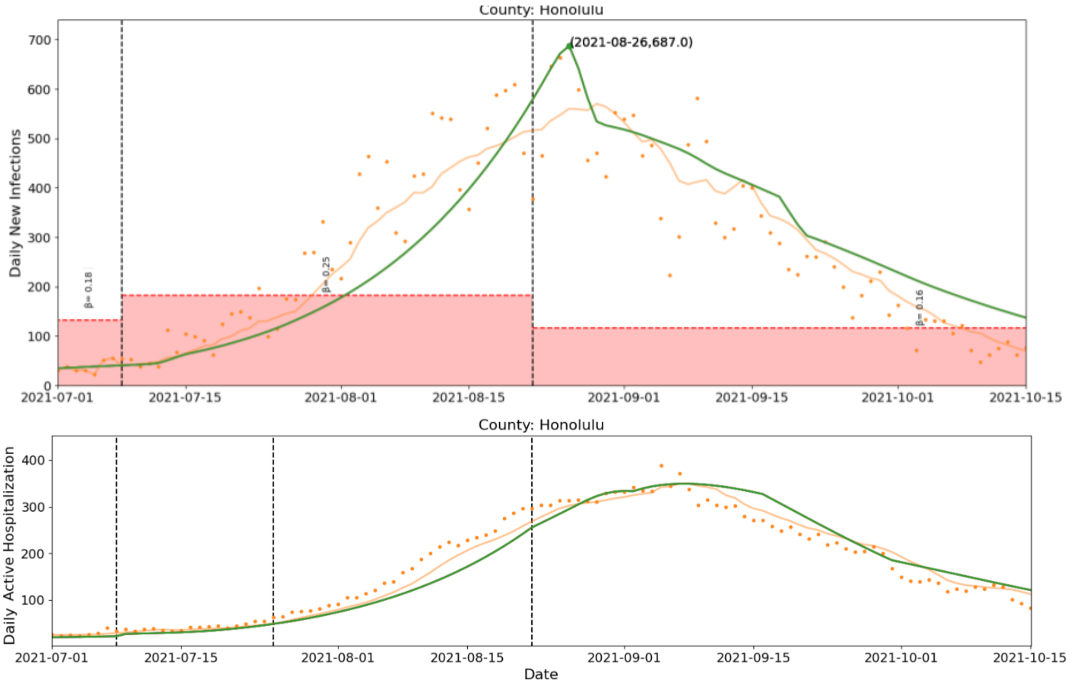

Figure 13. Honolulu County. Top plot is new daily cases and bottom plot is active hospitalization. The peak for reported DOH cases was 687 on August 24 and 389 on September 4 for active hospitalization.

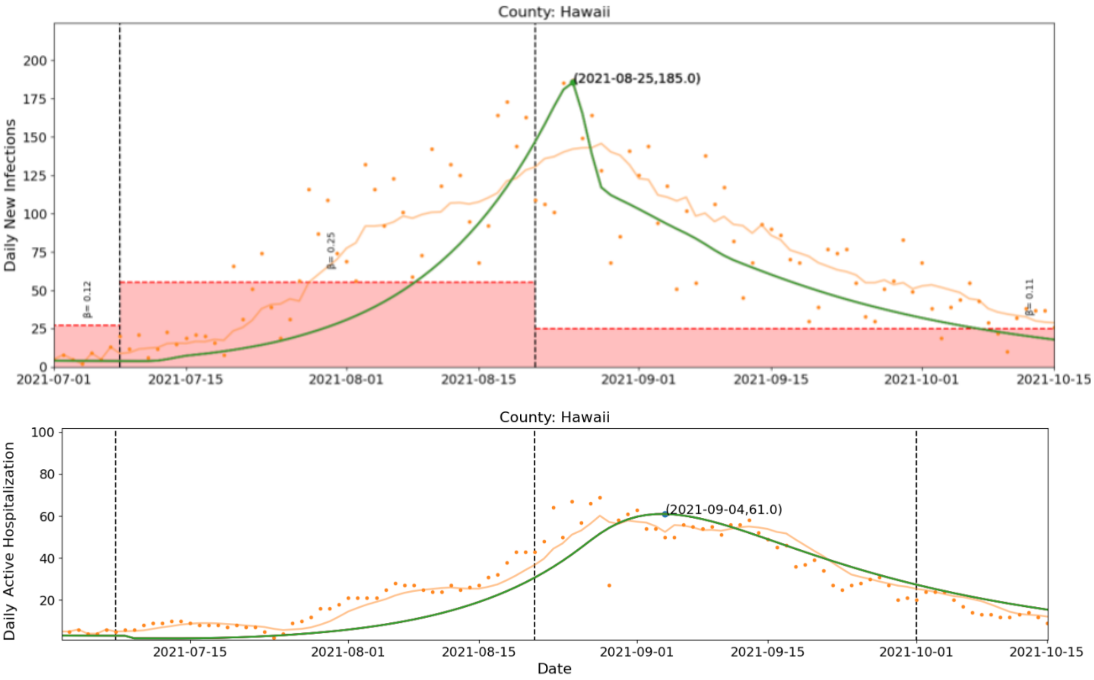

Figure 14. Hawai'i county. New daily cases (top) and active hospitalizations (bottom) for the period July-October 2021. The peak for reported DOH cases was 187 on August 24 and 61 on August 27 active hospitalizations.

Table 6. L_2 distance to measure the error of the model fit with respect to real data - Delta Period.

County	L_2 distance between model fit and actual data (ni, hosp)	L_2 distance between model fit and 7 day average of actual data(ni, hosp)
Honolulu	0.373, 0.286	0.276, 0.167
Hawai‘i	0.404, 0.373	0.159, 0.244
Maui	0.368, 0.497	0.222, 0.424
Kaua‘i	1.355, 3.364	1.292, 3.354

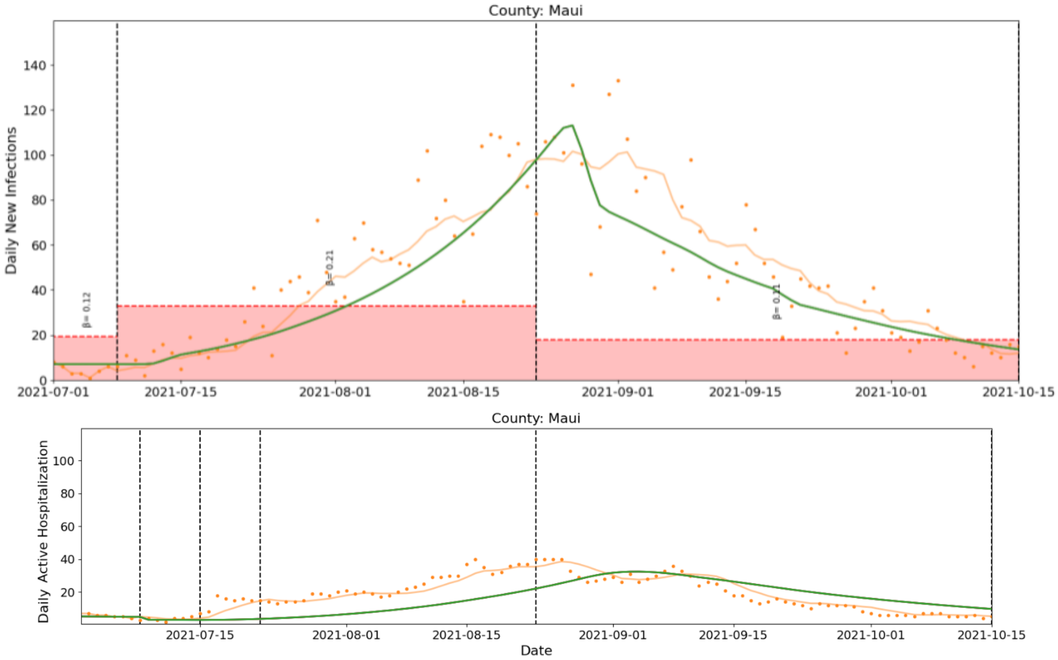

Figure 15. Maui County. New daily cases (top) and active hospitalizations (bottom) for the period July-October 2021. The peak for reported DOH cases was 133 on August 31 and 40 on August 25 for active hospitalization.

Figure 17 shows the count of new daily cases under the current vaccination rates but without the appearance of the Delta mutation. The green curve is the actual model fit for the reported data from the DOH, whereas the blue curve is a projection of new daily cases that would have occurred if the transmission would have been kept as the one of the Alpha variant i.e. no Delta variant. It is clear that the vaccination would have then been enough to flatten the curve and avoid a surge.

4.3. *Omicron variant B.1.1.529*

The B.1.1.529 variant, Omicron, was first reported to WHO from South Africa on November 24, 2021. The first known case of this more contagious variant was confirmed in the state of Hawai‘i on December 5, 2021. Based on estimates from the literature [4, 38], we assume that the original Omicron strain BA.1 is 2.4 times more transmissible than the Delta variant B.1.617.2 (more than 5 times transmissible than the original strain). Omicron's subvariant BA.2 was detected shortly after

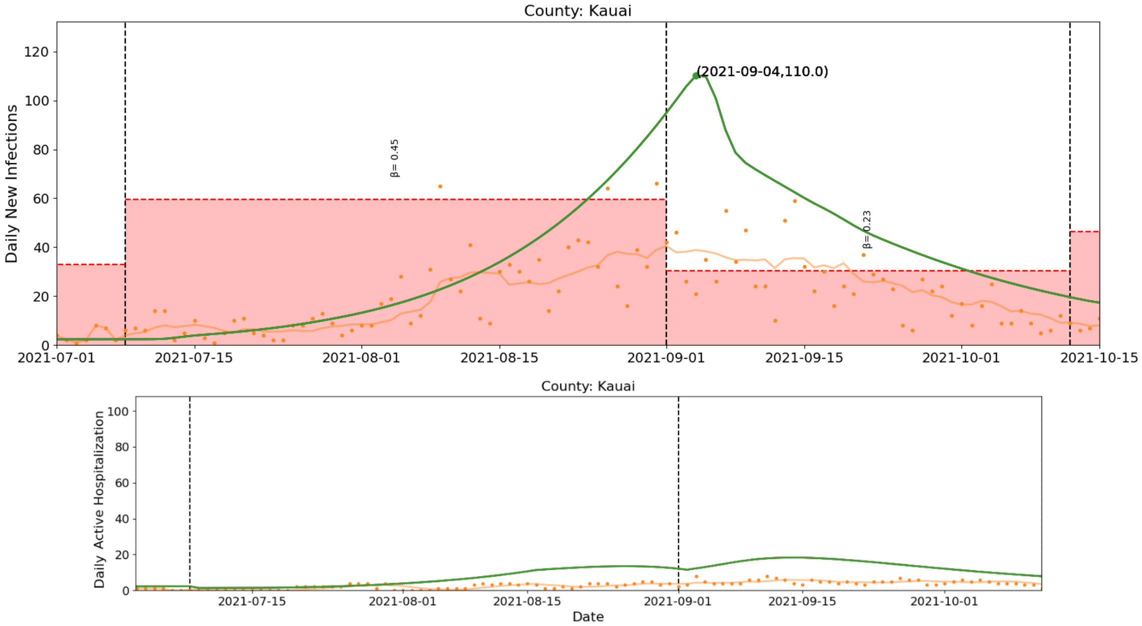

Figure 16. Kauaʻi County. New daily cases (top) and active hospitalizations (bottom) for the period July-October 2021. The peak for reported DOH cases was 66 on August 31 and for active hospitalization was 8 on September 11.

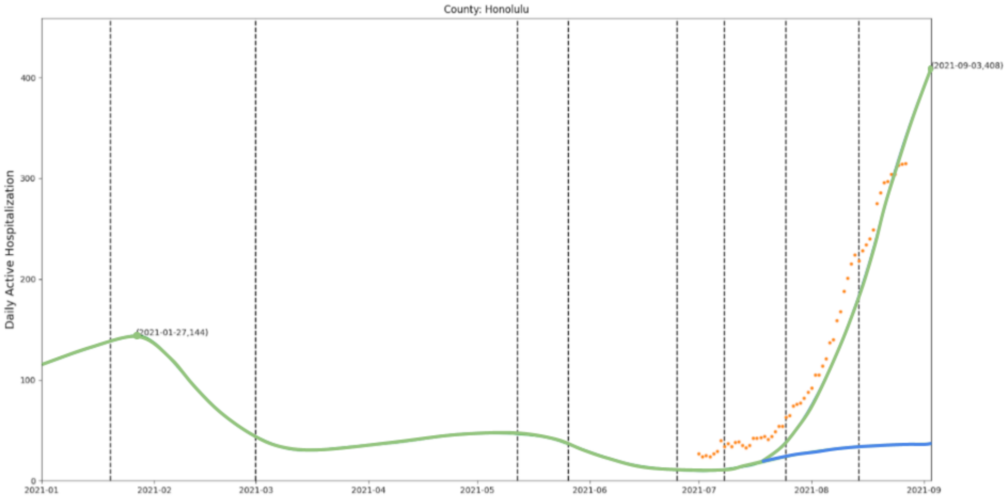

Figure 17. The green curve shows the actual fit with the Delta variant and the blue curve shows the hypothetical scenario for summer 2021 corresponding to not having the Delta variant.

and is assumed to be 1.5 times more transmissible than the original Omicron strain BA.1 (about 8 times more transmissible than the original Covid-19 strain). As the Omicron variant appeared in the state of Hawaiʻi the model was updated to include multiple variants, as described in Section 2. In this section we present the chronological order in which the modeling was used to assess the situation as the Omicron variant was spreading in the state of Hawai‘i and to provide forecasts as a resource to the Government and the media. We highlight only the most important HiPAM reports and their results, other reports can be found on the HiPAM website [18].

HiPAM report of December 7, 2021. This was the first report incorporating the Omicron variant. It showed that Honolulu was plateauing and not decreasing despite the safe access program in place and the Honolulu County vaccination level increasing to 75%, as of December 2021, from about 60% back in June 20, 2021. This illustrated that the county was displaying a significantly higher transmission of the virus among individuals. The other counties did not have yet confirmed detection of variant BA.1, but the corresponding data also required an increase in the transmission rate to optimize the fit. Figure 18 (from that report) represents the total number of infected symptomatic individuals (summing all I compartments in the model) versus the total number of infected asymptomatic individuals (summing all E compartments in the model) for Honolulu County. Each loop represents a different phase of the pandemic: Mar 22, 2020 - June 1, 2020 (Black), June 2,2020 - Oct 23, 2020 (Blue), Oct 24, 2020 - Mar 3, 2021 (Green), Mar 4, 2021 - June 25, 2021(Yellow), June 26, 2021 - Nov 14, 2021 (Red) and most importantly we could see the birth of a new loop starting around Nov 15, 2021 (Purple), that turned out to be the beginning of the Omicron surge. Note that prior to the Delta variant there were about 5 asymptomatic infections for every symptomatic infection, while during the Delta period there were 16-17 asymptomatic individuals for every symptomatic individual, a ratio which continued during the Omicron phase. This is likely a consequence of the vaccination preventing symptoms.

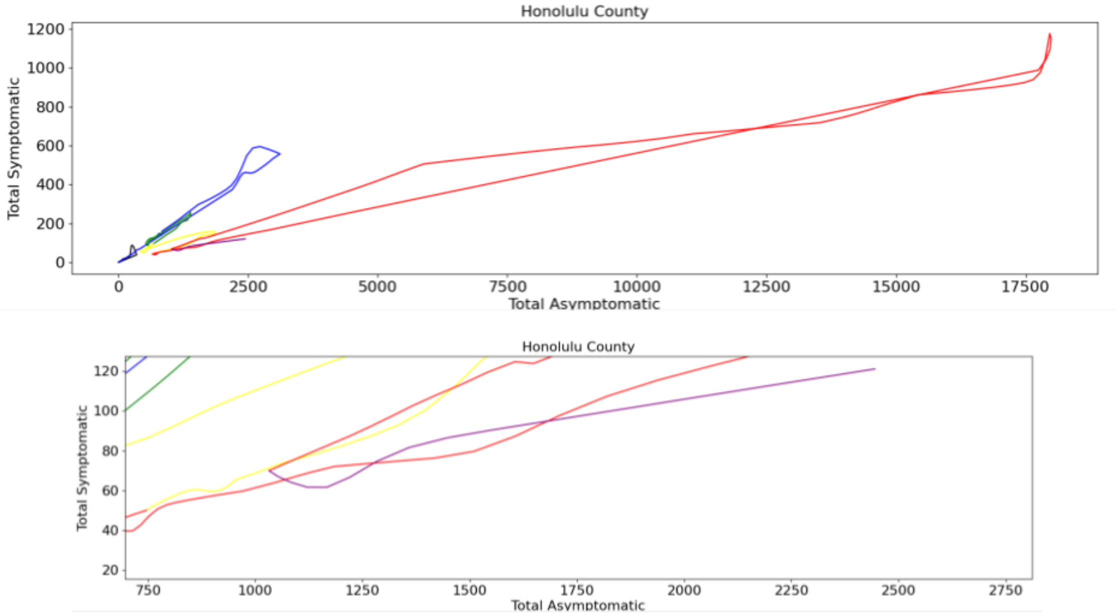

Figure 18. Total Symptomatic versus Total Asymptomatic. Bottom plot is a zoom to show the beginning of a new loop (Omicron). It can be seen two different slopes for the loops, one prior to Delta variant and one after likely due to the fact that vaccination increased the rate of asymptomatic cases versus symptomatic ones.

HiPAM report of December 19, 2021. This report introduced for the first time cones of uncertainties in our forecasts, which was motivated by uncertainties about the increase in transmission with the Omicron mutation versus the prior ones, uncertainties of the exact impact of vaccines and new mutations on hospitalization rates, as well as uncertainties due to rapid changes in people's behavior in response to the number of reported daily cases by the DOH. The Forecast from our model estimated that on January 2, 2022 we would have 4,422 new daily cases in Honolulu County with an uncertainty bracket of [2,235;9,604] (large due to the exponential nature of the phenomenon). The forecast assumed a constant vaccination rate based on the latest data as well as a slight change in people's behavior due to the holidays but it does not assume any change in mitigation measures.

HiPAM report of December 26, 2021. The model included the Omicron variant for all counties, since it was then officially detected everywhere. Honolulu County was forecast to be on a similar trajectory as predicted on December 19, while the forecast for new daily cases on January 2, 2022 was at 279, 305 and 144 for Hawai‘i, Maui and Kaua‘i counties, respectively. On January 4, 2022, the DOH dashboard reported a 7 day-average of 2,061 for Honolulu County, 263 for Hawai‘i County, 352 for Maui County and 130 for Kaua‘i County. Note that Honolulu County had shortages of testing capabilities during the holidays and on January 4, 2022 the new daily cases in Honolulu were reported as 3,447 and 3,886 on January 11, 2022. The predictions of the model proved to be extremely accurate despite all uncertainties around the Omicron mutation at that stage of the pandemic. Our forecasts predicted ahead of time the peak of the Omicron surge to be around the second (Honolulu) and third (Hawai‘i, Maui and Kaua‘i) week of January 2022 which turned out to be quite accurate as well. Importantly, the forecast highlighted that, based on early information about the Omicron mutation and estimates for the state of Hawai‘i hospitalizations would not see a surge as it was the case in July of 2021 despite the higher new daily cases.

HiPAM report of February 17, 2021. The report highlighted that both new daily cases and hospitalizations were on a downward trend and forecast that the rapid initial decrease was starting to taper off. Continuous assessment was needed however due to the emergence of Omicron BA.2. Additionally, an increased use of at home testing may have resulted in decreased official DOH COVID-19 case counts. The simulations at the time showed that hospitalizations rates we changing gradually. We suspect it is due to the fact that early in the Omicron surge a part hospitalizations were still caused by the Delta variant. Then, as the Omicron variants became dominant hospitalization rates fell to lower levels.

HiPAM report of April 12, 2021. In Figures 19 to 22 we display the reported data from the DOH as well as the model fit from November 1, 2021 to April 30, 2022, both for new daily cases and for hospitalizations. The model included two co-existence variants, BA.1 and BA.2 (both dominant starting mid-December 2021 over any prior variant), vaccine fading, and renewed susceptibility for individuals with prior infection due to waning immunity after some period. Note that the cones of uncertainty are provided in those figures. The Omicron surge did coincide with limited testing capabilities as well as the introduction of at-home testing (COVID Test At-Home Testing Challenge provided 125,000 O'ahu residents who live in eligible ZIP codes with eight rapid antigen tests as a pilot program and it was then implemented in the state for everyone in mid-January 2022). As a result, many positives cases were not reported to the DOH, which created a biased assessment of the situation. For this reason, we used hospitalizations as a benchmark for our fit. It can be seen on the figures that the model fits hospitalizations well while it is overshooting the DOH reported daily cases. We do believe that because of the under-count of daily cases due to the testing issues, our model provides a better representation of what was the actual situation. Table 7 provide the L_2 distance between our model fit and reported data.

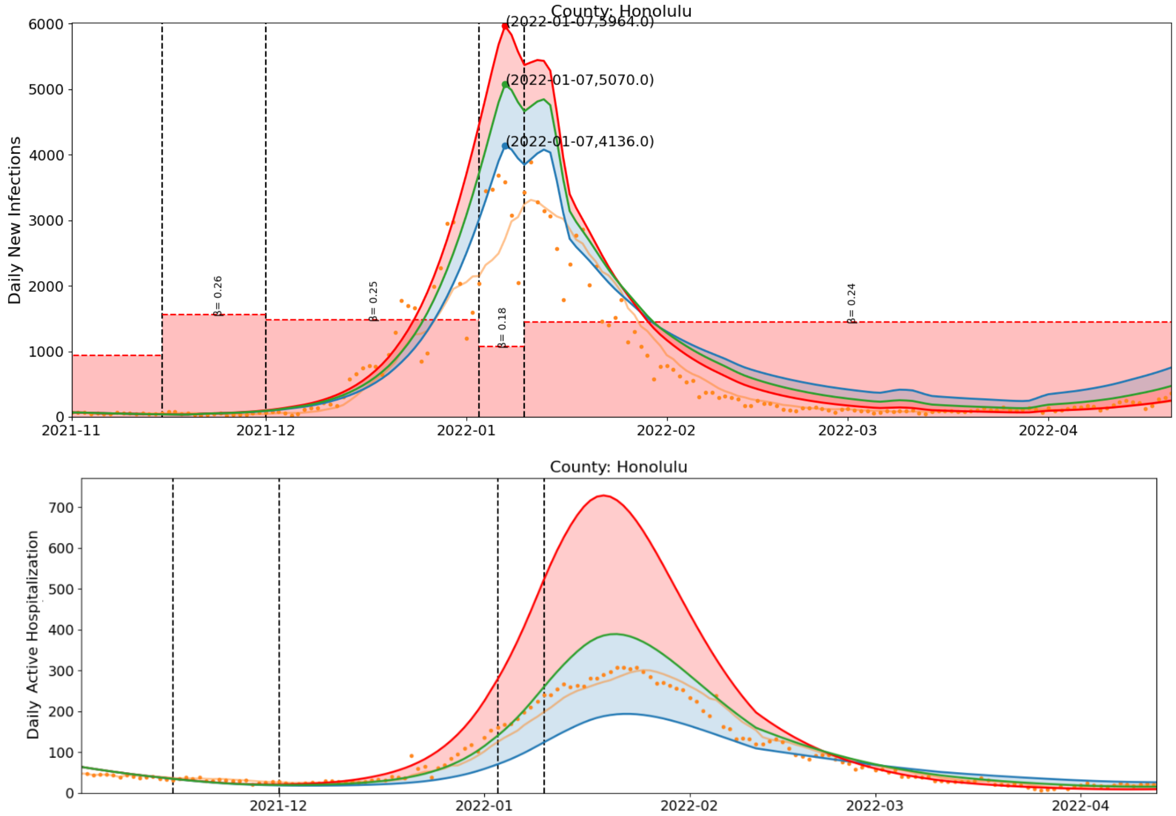

Figure 19. Honolulu County. New daily cases (top) and active hospitalizations (bottom) for the period November 2021-April 2022. The peak for reported DOH cases was 3,884 on January 11, 2022 and for active hospitalization was 307 on January 24, 2022. The green curve is the optimized fit. The red and blue curve are the worst and the best estimates giving a cone of uncertainty for the forecasts. The red (blue) curve assumes a variant transmission rate that is higher (lower) by 0.1 and parameter r_2 that is higher(lower) by 0.05. The dotted vertical lines represent the dates at which the transmission rate is adjusted. The red rectangles show the optimized transmission rates for the corresponding duration.

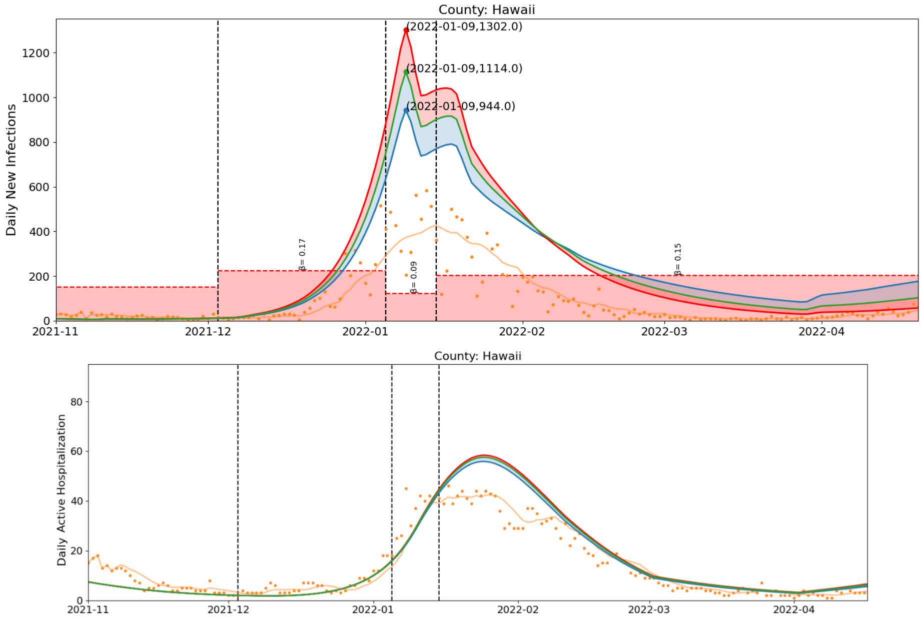

Figure 20. Hawai‘i County. New daily cases (top) and active hospitalizations (bottom) for the period November 2021-April 2022. The peak for reported DOH cases was 582 on January 12, 2022 and for active hospitalization was 46 on January 17, 2022. See Figure 19 for a description of the various curves.

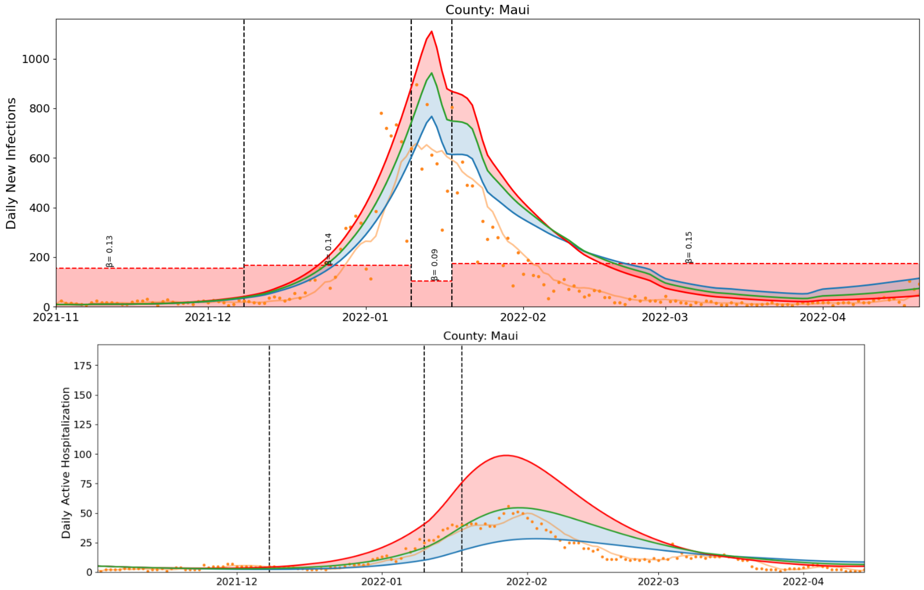

Figure 21. Maui County. New daily cases (top) and active hospitalizations (bottom) for the period November 2021-April 2022. The peak for reported DOH cases was 895 on January 11, 2022 and for active hospitalization was 56 on January 28, 2022. See Figure 19 for a description of the various curves.

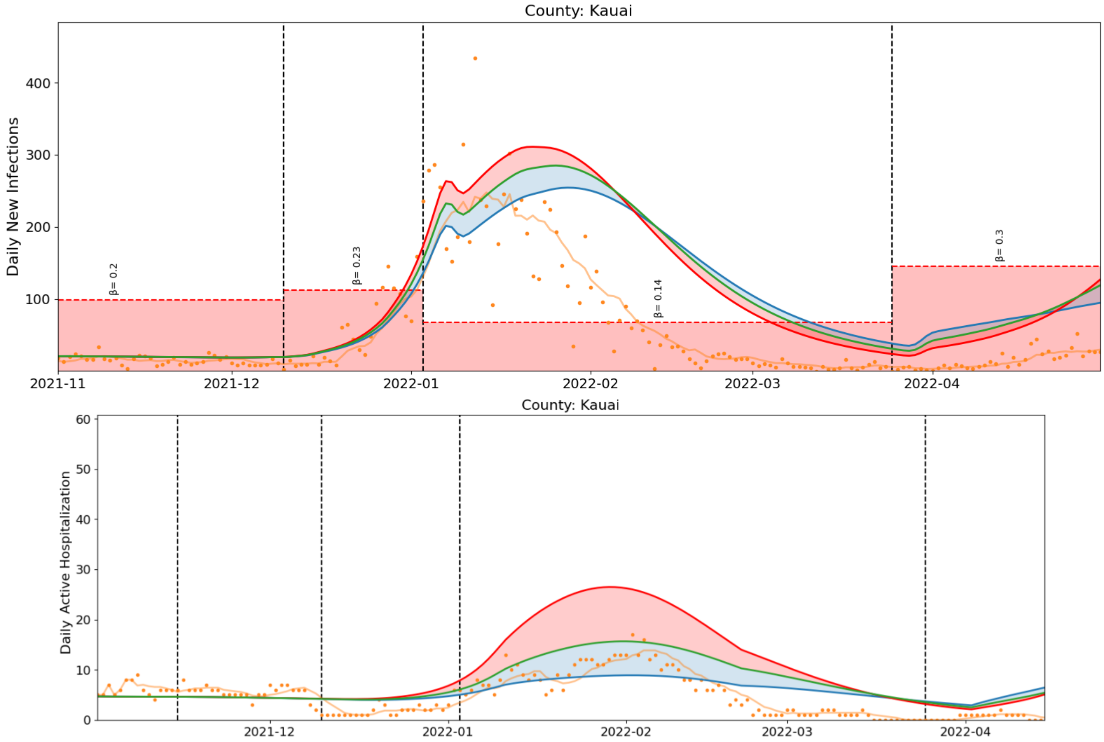

Figure 22. Kaua'i County. New daily cases (top) and active hospitalizations (bottom) for the period November 2021-April 2022. The peak for reported DOH cases was 436 on January 12, 2022 and for active hospitalization was 17 on February 2, 2022. See Figure 19 for a description of the various curves.

Table 7. L_2 distance to measure the error of the model fit with respect to real data - Omicron Period.

County	L_2 distance between model fit and actual data (ni,hosp)	L_2 distance between model fit and 7 day average of actual data(ni,hosp)
Honolulu	(0.337,0.284)	(0.326,0.284)
Hawai'i	(0.445,0.356)	(0.436,0.333)
Maui	(0.379,0.395)	(0.325,0.365)
Kaua'i	(0.428,0.486)	(0.480,0.486)

Figure 23 illustrates the fact that the delay between the curves for new daily cases and active hospitalization evolved during the pandemic by showing active hospitalization versus new daily infections. The flatter slope of the loop for the Omicron indicates that less infected individuals were getting hospitalized as compared to prior variants. We also ran estimates on actual data, which showed that the delay between new daily cases and hospitalizations was about 14 days at the beginning of the pandemic and got shortened to about 9 days with the Omicron phase.

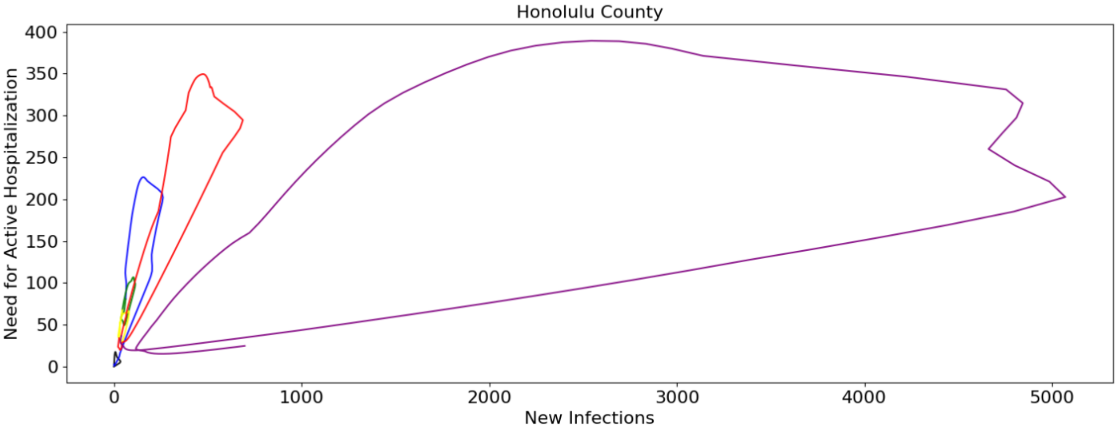

Figure 23. Plot to show differences in ratio of hospitalizations versus new daily cases for various surges.

Table 8. This Table highlights the major assumptions for the model. *: infections for the new mutations were introduces as a mix of asymptomatic and symptomatic cases in the multi-variants model. The dates in introduction of the new variants were determine to optimize the fit.

Omicron BA.1	$\mho_{factor} = 5.28$
Omicron BA.2	$\mho_{factor} = 7.92$
ω	0.24 (more breakthrough cases with Omicron)
Vaccine Fading	Introduced from Dec 1, 2021 as explained in Section 2 (one year after first shot was implemented, second shot over summer).
Re-susceptibility to infection	As explained in Section 2 it follows the rate of infection with a delay of six months. Re-susceptibility is starting in our model on February 15, 2022. Cases before the Delta surge were small and we neglect them for re-infection.
Masks	Masks Mandate has been removed from the model on March 26, 2022 following the State's rules.
Safe Travel	Safe Travel program has been removed on March 25, 2022. Travelers are then assumed to be incoming with a percentage of infection identical to the US average.
Safe Access	Safe Access has been removed in Honolulu County on March 6, 2022 and in Maui County on February 21, 2022 following each county's rule.
Honolulu	Omicron BA.1 cases were added in the model November 13, 2021 and Omicron BA.2 cases on December 20, 2021.*
Hawai'i	Omicron BA.1 cases were added in the model December 2, 2021 and Omicron BA.2 cases on December 20, 2021.*
Maui	Omicron BA.1 cases were added in the model December 2, 2021 and Omicron BA.2 cases on December 27, 2021.*
Kaua'i	Omicron BA.1 cases were added in the model December 5, 2021 and Omicron BA.2 cases on December 27, 2021.*

Table 8 summarizes our parameter assumptions. The introduction of the new mutations in the multi-variant model requires some careful thinking. Introducing a single case of a new variant will not allow for its spreading. Instead, we used the variant reports to introduce cases in various compartments of our model to fit the reported data, and the date of introduction of the variant was used to optimize the fit. Adjustments in people's behavior due to the Holidays and gatherings were also taken into account. Table 9 provides the hospitalization rates for the period from November 1, 2021 to April 30, 2022.

Table 9. Hospitalization rates(σ_1, σ_2) for four counties.

Dates	Honolulu(σ_1, σ_2)	Hawai'i(σ_1, σ_2)	Maui(σ_1, σ_2)	Kaua'i (σ_1, σ_2)
	(5%,10%)	(4.5%,9%)	(4%,8%)	(2%,4%)
Nov 12 - Dec 15	(5%,10%)	ramp down	(4%,8%)	(2%,4%)
Dec 16 - Jan 9	(5%,10%)	ramp down	ramp down	(2%,4%)
Jan 10 - Feb 9	(5%,10%)	ramp down	(5.25%,2.625%)	ramp down
Feb 10 - Mar 19	(4.5%,2.25%)	ramp down	(5.25%,2.625%)	ramp down
Feb 20 - Mar 1	(4.5%,2.25%)	ramp down	(5.25%,2.625%)	(1.5%,0.75%)
Mar 2 - Apr 1	(4.5%,2.25%)	(1.5%,0.75%)	(5.25%,2.625%)	(1.5%,0.75%)

5. Discussion

In this paper, using our discrete generalized SEIR model tailored specifically to the state of Hawai'i, we illustrated the evolution of the pandemic within an island chain environment that did not completely close its borders to travelers, as opposed to many other island nations. As a result, the new infectious SARS-CoV-2 virus and its follow-up mutations spread among the population. Two important phases are described in detail: the Delta and the Omicron surges.

Phase 1: During the Spring of 2021, COVID-19 variant cases declined in Hawai'i, except for the Delta variant. The optimized transmission rate β in the model multiplied by the variant transmissibility $\mho_{factor}$ was roughly double what it was a year earlier, with cases climbing rapidly despite vaccinations. Forecasting predicted about 3,000 known cases along with 16,000 asymptomatic infections in Honolulu County by October 2021. However, due to these predictions, mitigation measures were put in place, including social distancing, restrictions on gathering numbers, and reduced travel. Honolulu implemented the safe access program on September 13, requiring all employees of businesses, such as restaurants, gyms, and similar establishments to show proof of vaccination or a negative test result each week. Ultimately 3,000 cases per day in Honolulu County was not reached at that time and the model prediction was defeated thanks to the mitigation measures.

Phase 2: After plateauing for a couple of months, model estimates at the start of December indicated that we could be at the early part of a surge caused by the recent Omicron variant. The forecasts predicted a similar course as for Delta, with new daily cases exceeding 3,000 by February 2022. While the safe access program was still in place during the surge of the Omicron variant, other mitigation measures, such as restricting gathering size, and social distancing, started to relax. At the same, time the model estimated a smaller surge in active hospitalizations. As a result, no restrictions in mitigation measures were taken and daily new cases exploded following the models predictions. However, the impact on bars, restaurant industry and the tourism sector in general was much less pronounced during the Omicron surge, which slowed-down further damages to Hawai‘i’s economy.

Figures 24a and 24b summarize the evolution of new daily cases and hospitalization for the first two years of the pandemic, including the two phases described above. Both sets of data are normalized by the largest magnitude in their timeline, so the fact that the curve for the daily new cases is significantly wider in early 2022 shows just how dramatic the spike in numbers was for Omicron as compared to Delta. However, the surges in active hospitalizations are quite comparable, with Delta occurring first between August and October of 2021. Figure 24c shows cumulative deaths.

In addition to providing a good fit to reported data from the DOH, our model has proven to be well aligned with the CDC findings reported in [1] on April 26, 2022. Indeed, the CDC stated that estimated 58% of Americans have been infected with SARS-CoV-2. For the state of Hawai‘i, our model estimated that on April 15, 2022 about 62% of Honolulu County population was infected, 61% for Hawai‘i County and 59% for Maui County. As shown with the estimates for the total number of infections, the structure of the model allows for estimations of quantities that cannot be directly measured, such as the daily number of asymptomatic infected individuals. Table 10 provides some of those numbers for all four counties.

Table 10. Cumulative numbers that cannot be inferred from reported data by the DOH. They span the beginning of the pandemic to April 30, 2022.

County	Cumulative Number of Infections (both Symptomatic and Asymptomatic)	Cumulative Number of Infected Asymptomatic Individuals	Cumulative Number of Vaccinated Individuals (at least 2 doses) that have been Infected
Honolulu	625,607	426,387	413,746
Hawai‘i	124,703	84,185	79,079
Maui	101,511	64,605	57,237
Kaua‘i	65,092	46,726	33,190

After April 30, 2022 reported daily cases by the DOH for all counties showed a slight upward trend, followed quickly by plateauing, and as of September 2022, a downward trend. BA.5 and BA.4 variants, considered to be especially efficient spreaders of the disease, were first detected by experts in early 2022 and confirmed to be in all four major counties of Hawai‘i in June 2022, but their impact is unclear for several reasons, including people not testing, or testing and not reporting, as well as DOH limiting access to data. Indeed, at the end of Spring 2022 the DOH stopped reporting numbers daily and then later stopped reporting active hospitalizations per counties. The limitations of data made it impossible for us to understand how the model was performing after that point.

Overall, this paper shows that a model which is well calibrated to the specifics of a geographically isolated environment can be a useful tool in assessing the spread of one or many competing viral pathogens. Moreover, it demonstrates that the initial choice of a reasonably flexible model structure allows one to start with a simpler model and gradually evolve it along with the pandemic.

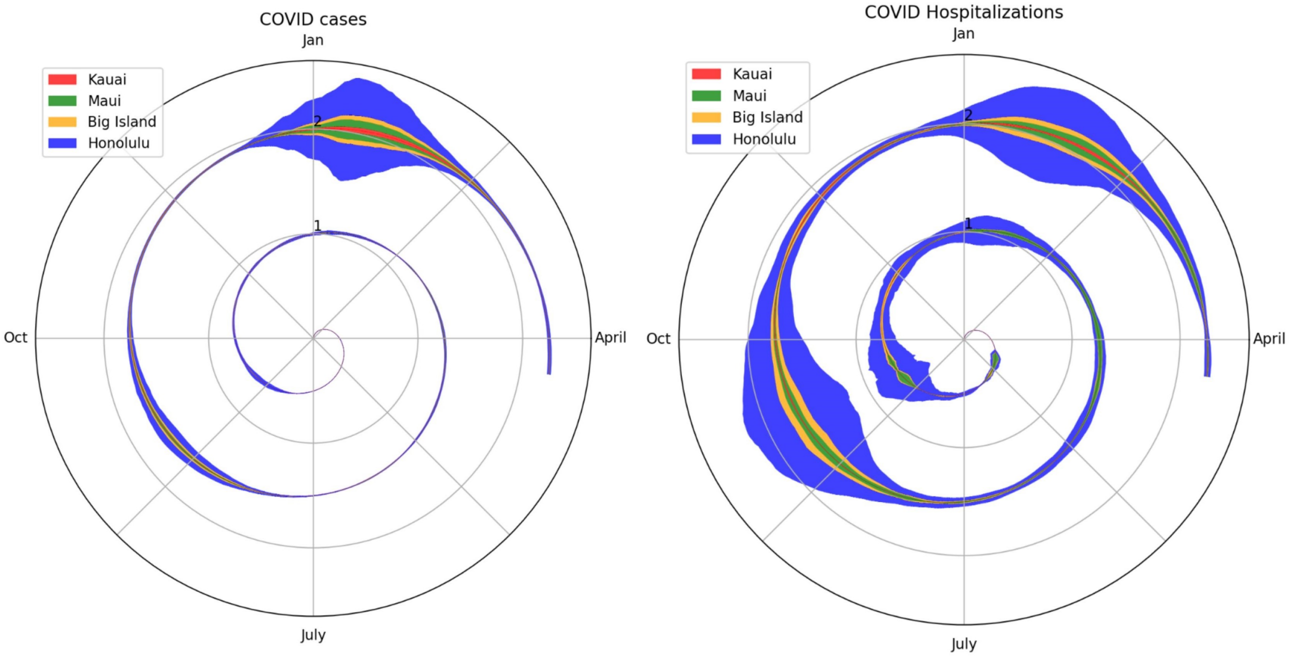

(a) Average Daily New Cases

(b) Average Active Hospitalizations

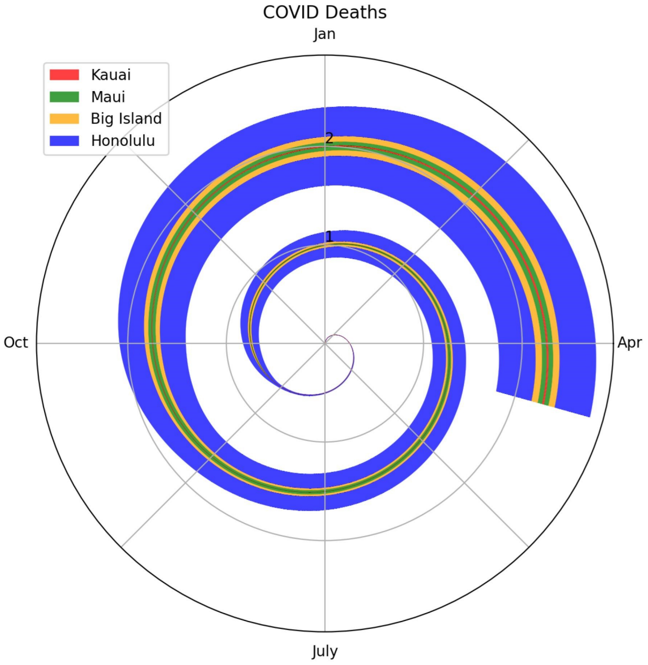

(c) Total Death for Hawai‘i

Figure 24. Two years of DOH data, separated into the 4 counties.

Acknowledgments

This material is based upon work supported by the National Science Foundation under Grant No. 2030789. The authors also gratefully acknowledge support from the Coronavirus State Fiscal Recovery Funds via the Governor's Office Hawai'i Department of Defense and the University of Hawai'i at Manoa Provost's Office. Finally, the authors also gratefully acknowledge support from the members of the Hawaii Pandemic Applied Modeling Work Group.

Conflict of interest

The authors declare no conflict of interest.

References

1. American Hospital Association: CDC estimates 58% of Americans have been infected with SARS-CoV-2, Apr. 26, 2022. Available from: `https://www.aha.org/news/headline/2022-04-26-cdc-estimates-58-americans-have-been-infected-sars-cov-2`
2. S. Allred, M. Chyba, J. M. Hyman, Y. Mileyko, B. Piccoli, The COVID-19 Pandemic Evolution in Hawai'i and New Jersey: A Lesson on Infection Transmissibility and the Role of Human Behavior, *Predicting Pandemics in a Globally Connected World*, **1** (2022), 109–140. https://doi.org/10.1007/978-3-030-96562-4_4
3. N. Bellomo, M. A. J. Chaplain, Predicting Pandemics in a Globally Connected World, Volume 1 Toward a Multiscale, Multidisciplinary Framework through Modeling and Simulation, Springer International Publishing, 2022. https://doi.org/10.1007/978-3-030-96562-4
4. Bloomberg: Omicron Four Times More Transmissible Than Delta in New Study, By Kanoko Matsuyama, Dec. 8, 2021. Available from: https://www.bloomberg.com/news/articles/2021-12-09/omicron-four-times-more-transmissible-than-delta-in-japan-study
5. C. Branas, A. Rundle, S. Pei, W. Yang, B. G. Carr, S. Sims, et al., Flattening the curve before it flattens us: hospital critical care capacity limits and mortality from novel coronavirus (SARS-CoV2) cases in US counties, *medRxiv*, 2020.
6. D. Buitrago-Garcia, D. Egli-Gany, M. J. Counotte, S. Hossmann, H. Imeri, A. M. Ipekci, et al., Occurrence and transmission potential of asymptomatic and presymptomatic SARS-CoV-2 infections: A living systematic review and meta-analysis, *PLOS Med.,* **17** (2020), e1003346. https://doi.org/10.1371/journal.pmed.1003346
7. M. Chyba, Y. Mileyko, O. Markovichenko, R. Carney, A. Koniges, Epidemiological Model of the Spread of COVID-19 in Hawaii's Challenging Fight Against the Disease, *The Ninth International Conference on Global Health Challenges*, (2020), 32–38.
8. M. Chyba, T. Klotz, Y. Mileyko, C. Shanbrom, A look at endemic equilibria of compartmental epidemiological models and model control via vaccination and mitigation, *arXiv: 2109.01738*, 2021.

9. M. Chyba, P. Kunwar, Y. Mileyko, A. Tong, W. Lau, A. Koniges, COVID-19 heterogeneity in islands chain environment, *PLoS One,* **17** (2022), e0263866. https://doi.org/10.1371/journal.pone.0263866

10. N. M. Ferguson, D. Laydon, G. Nedjati-Gilani, N. Imai, K. Ainslie, M. Baguelin, et al., Report 9 - Impact of non-pharmaceutical interventions (NPIs) to reduce COVID-19 mortality and healthcare demand, *Imperial College London*, **10** (2020), 491–197.

11. M. Gatto, E. Bertuzzo, L. Mari, S. Miccoli, L. Carraro, R. Casagrandi, et al., Spread and dynamics of the COVID-19 epidemic in Italy: Effects of emergency containment measures, *Proceedings of the National Academy of Sciences*, **117** (2020), 10484–10491. https://doi.org/10.1073/pnas.2004978117

12. G. Giordano, F. Blanchini, R. Bruno, P. Colaneri, A. Di Filippo, A. Di Matteo, et al., Modelling the COVID-19 epidemic and implementation of population-wide interventions in Italy, *Nat. Med.,* **26** (2020), 855–860. https://doi.org/10.1038/s41591-020-0883-7

13. W. T. Harvey, A. M. Carabelli, B. Jackson, R. K. Gupta, E. C. Thomson, E. M. Harrison, et al., SARS-CoV-2 variants, spike mutations and immune escape, *Nat. Rev. Microbiol.*, **19** (2021), 409–424. https://doi.org/10.1038/s41579-021-00573-0

14. Hawaii Department of Health, Disease Outbreak Control Division: COVID-19 Dashboard. Available from: https://health.hawaii.gov/coronavirusdisease2019

15. Hawaii Population Model. *Hawai'i Data Collaborative, Department of Health, Disease Outbreak Control Division:* COVID-19 Data Reports, 2022. Available from: https://health.hawaii.gov/coronavirusdisease2019/what-you-should-know/covid-19-data-reports

16. Hawai'i Department of Health: Vaccination Distribution Plan, 2022. Available from: www.hawaiicovid19.com/wp-content/uploads/2021/01/Executive-Summary_Final1_010721.pdf

17. Hawaii News Now: Ventilators from Hawaii's emergency stockpile now in use as more relief nurses are on their way, By Allyson Blair, Aug. 25, 2021. Available from: https://www.hawaiinewsnow.com/2021/08/26/ventilators-emergency-stockpile-now-use-more-relief-nurses-are-their-way/

18. Hawai'i Pandemic Applied Modeling Work Group, 2022. Available from: www.hipam.org

19. H. W. Hethcote, The Mathematics of Infectious Diseases, *SIAM Rev.*, **42** (2000), 599–653. https://doi.org/10.1137/S0036144500371907

20. Honolulu Star-Advertiser: Hawaii's daily COVID cases are forecast to peak at 3,700 in October, By Nina Wu, Aug. 23, 2021. Available from: https://www.staradvertiser.com/2021/08/23/hawaii-news/hawaiis-daily-covid-cases-are-forecast-to-peak-at-3700-in-october/

21. Honolulu Star-Advertiser: Kaiser postpones elective surgeries and procedures on Oahu, Maui due to COVID surge, By Nina Wu, Aug. 27, 2021. Available from: https://www.staradvertiser.com/2021/08/27/breaking-news/kaiser-postpones-elective-surgeries-and-procedures-on-oahu-maui-due-to-covid-surge/

22. Honolulu Star-Advertiser: No ICU beds available at Queen's medical facilities as COVID cases surge in Hawaii, By Sophie Cocke, Aug. 17, 2021. Available from:

https://www.staradvertiser.com/2021/08/17/hawaii-news/no-icu-beds-available-at-queens-medical-facilities-as-covid-cases-surge-in-hawaii/

23. A. D. Iuliano, J. M. Brunkard, T. K. Boehmer, E. Peterson, S. Adjei, A. M. Binder, et al., Trends in Disease Severity and Health Care Utilization During the Early Omicron Variant Period Compared with Previous SARS-CoV-2 High Transmission Periods — United States, December 2020–January 2022, *MMWR Morb. Mortal.,* **71** (2022), 146–152. https://doi.org/10.15585/mmwr.mm7104e4

24. V. Kala, K. Guo, E. Swantek, A. Tong, M. Chyba, Y. Mileyko, et al., Pandemics in Hawai'i: 1918 Influenza and COVID-19, *The Ninth International Conference on Global Health Challenges*, (2020), 26–31.

25. D. G. Kendall, Deterministic and stochastic epidemics in closed populations, *University of California Press*, (2020), 149–166. https://doi.org/10.1525/9780520350717-011

26. W. O. Kermack, A. G. McKendrick, A contribution to the mathematical theory of epidemics, *R. Soc. Lond. A*, **115** (1927), 700–721. https://doi.org/10.1098/rspa.1927.0118

27. W. O. Kermack, A. G. McKendrick, Contributions to the mathematical theory of epidemics. II.—The problem of endemicity, *Proceedings of the Royal Society of London. Series A, containing papers of a mathematical and physical character*, **138** (1932), 55–83. https://doi.org/10.1098/rspa.1932.0171

28. P. Kunwar, O. Markovichenko, M. Chyba, Y. Mileyko, A. Koniges, T. Lee, A study of computational and conceptual complexities of compartment and agent based models, *Netw. Heterog. Media*, **17** (2022), 359–384. https://doi.org/10.3934/nhm.2022011

29. J. O. Lloyd-Smith, A. P. Galvani, W. M. Getz, Curtailing transmission of severe acute respiratory syndrome within a community and its hospital, *Proceedings of the Royal Society of London. Series B: Biological Sciences*, **270** (2003), 1979–1989. https://doi.org/10.1098/rspb.2003.2481

30. N. Ortega, M. Ribes, M. Vidal, R. Rubio, R. Aguilar, S. Williams, et al, Seven-month kinetics of SARS-CoV-2 antibodies and role of pre-existing antibodies to human coronaviruses, *Nat. Commun.,* **12** (2021), 1–10. https://doi.org/10.1038/s41467-021-24979-9

31. M. Park, A. R. Cook, J. T. Lim, Y. Sun, B. L. Dickens, A Systematic Review of COVID-19 Epidemiology Based on Current Evidence, *J. Clin. Med.,* **9** (2020), 967. https://doi.org/10.3390/jcm9040967

32. P. Qu, J. N. Faraone, J. P. Evans, Y. M. Zheng, L. Yu, Q. Ma, et al., Durability of Booster mRNA Vaccine against SARS- CoV-2 BA.2.12.1, BA.4, and BA.5 Subvariants, *New Engl. J. Med.,* **387** (2022), 1329–1331. https://doi.org/10.1056/NEJMc2210546

33. A. Richterman, E. A. Meyerowitz, M. Cevik, Indirect Protection by Reducing Transmission: Ending the Pandemic With Severe Acute Respiratory Syndrome Coronavirus 2 Vaccination, Open Forum Infectious Diseases *Open Forum Infectious Diseases*, **9(2)** (2022), ofab259. https://doi.org/10.1093/ofid/ofab259

34. R. Ross, H. P. Hudson, An Application of the Theory of Probabilities to the Study of a priori Pathometry. Part II, *Proceedings of the Royal Society of London Series A*, **93** (1917), 212–225. https://doi.org/10.1098/rspa.1917.0014

35. R. Ross, An Application of the Theory of Probabilities to the Study of a priori Pathometry. Part I, *Proceedings of the Royal Society of London Series A*, **92** (1916), 204–230. https://doi.org/10.1098/rspa.1916.0007
36. Y. B. Ruhomally, M. Mungur, A. A. H. Khoodaruth, V. Oree, M. Z. Dauhoo, Assessing the Impact of Contact Tracing, Quarantine and Red Zone on the Dynamical Evolution of the Covid-19 Pandemic using the Cellular Automata Approach and the Resulting Mean Field System: A Case study in Mauritius, *Appl. Math. Model.*, **111** (2022), 567–589. https://doi.org/10.1016/j.apm.2022.07.008
37. Science, Science Insider, Health: More people are getting COVID-19 twice, suggesting immunity wanes quickly in some, By Jop De Vrieze, Nov. 18, 2020. Available from: https://www.science.org/content/article/more-people-are-getting-covid-19-twice-suggesting-immunity-wanes-quickly-some
38. M. T. Sofonea, B. Roquebert, V. Foulongne, L. Verdurme, S. Trombert-Paolantoni, M. Roussel, et al., From Delta to Omicron: analysing the SARS-CoV-2 epidemic in France using variant-specific screening tests (September 1 to December 18, 2021) Cold Spring Harbor Laboratory Press, 2022. https://www.medrxiv.org/content/10.1101/2021.12.31.21268583v1
39. S. Sturniolo, W. Waites, T. Colbourn, D. Manheim, J. Panovska-Griffiths, Testing, tracing and isolation in compartmental models, *PLoS Comput. Biol.,***17** (2021), e1008633. https://doi.org/10.1371/journal.pcbi.1008633
40. State of Hawai'i Portal: Travel Data. Available from: https://hawaiicovid19.com/travel/data/
41. S. T. Tan, A. T. Kwan, I. Rodríguez-Barraquer, B. J. Singer, H. J. Park, J. A. Lewnard, et al., Infectiousness of SARS-CoV-2 breakthrough infections and reinfections during the Omicron wave, *medRxiv 2022.08.08.22278547*.
42. U.S. Bureau of Labor Statistics: Healthcare Population, May 2020, State Occupational Employment and Wage Estimates Hawaii. Available from: https://www.bls.gov/oes/current/oeshi.htm29-0000
43. U.S. Census Bureau. Available from: https://data.census.gov/cedsci/
44. F. Zhou, T. Yu, R. Du, G. Fan, Y. Liu, Z. Liu, et al., Clinical course and risk factors for mortality of adult inpatients with COVID-19 in Wuhan, China: a retrospective cohort study, *The Lancet*, **395** (2020), 1054–1062. https://doi.org/10.1016/S0140-6736(20)30566-3

AIMS Press